The terrible and great parton distributions

Pavel Nadolsky
Southern Methodist University
Dallas, TX, USA

Based on studies with
CTEQ-TEA and PDF4LHC
working groups

May 4, 2016

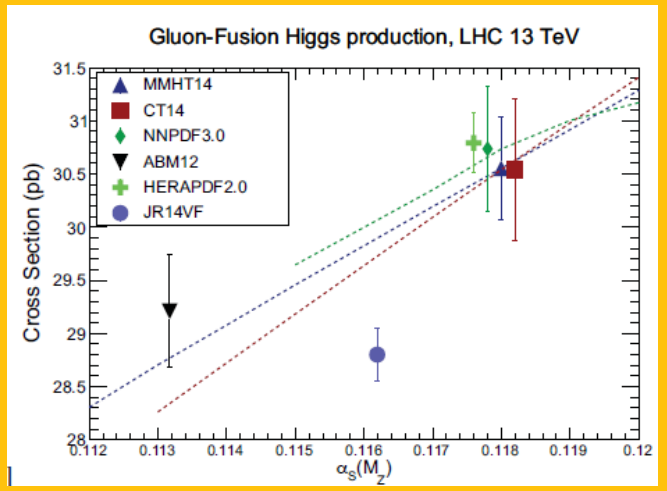

Parton distribution functions are basic blocks of theoretical predictions for hadronic scattering in perturbative QCD. They cannot be computed, but their accuracy must match accuracy of hard-scattering cross sections

Example: total cross section for gg → Higgs → $\gamma\gamma$

Cross section $\sigma_{pp\to H\to\gamma\gamma}$ for production and decay of H, e.g., via $g + g \to H$:

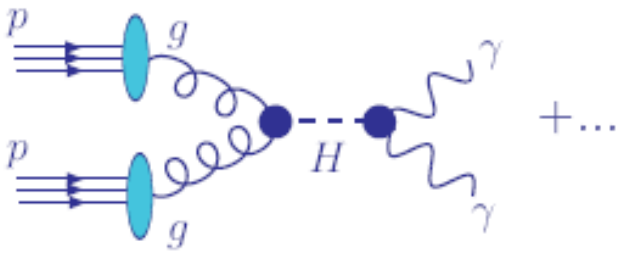

$$\sigma_{pp\to H\to\gamma\gamma X}(Q) = \sum_{a,b=g,q,\bar{q}} \int_0^1 d\xi_a \int_0^1 d\xi_b \hat{\sigma}_{ab\to H\to\gamma\gamma}\left(\frac{x_a}{\xi_a}, \frac{x_b}{\xi_b}, \frac{Q}{\mu_R}, \frac{Q}{\mu_F}; \alpha_s(\mu_R)\right)$$
$$\times f_a(\xi_a, \mu_F) f_b(\xi_b, \mu_F) + O\left(\frac{\Lambda_{QCD}^2}{Q^2}\right)$$

- The hard cross section $\hat{\sigma}_{ab\to H\to\gamma\gamma}$ can be computed as a **perturbative** series in $\alpha_s(\mu_R)$, at a renormalization scale $\mu_R \gg \Lambda_{QCD}$
- The PDFs $f_{a/p}\,(\xi, \mu_F)$ are **nonperturbative** functions associated with probabilities for finding a parton a with the momentum fraction ξ in the proton p, at a factorization scale $\mu_F \gg \Lambda_{QCD}$

Hard-scattering cross sections for $gg \to H \to \gamma\gamma$

N3LO for total cross sections

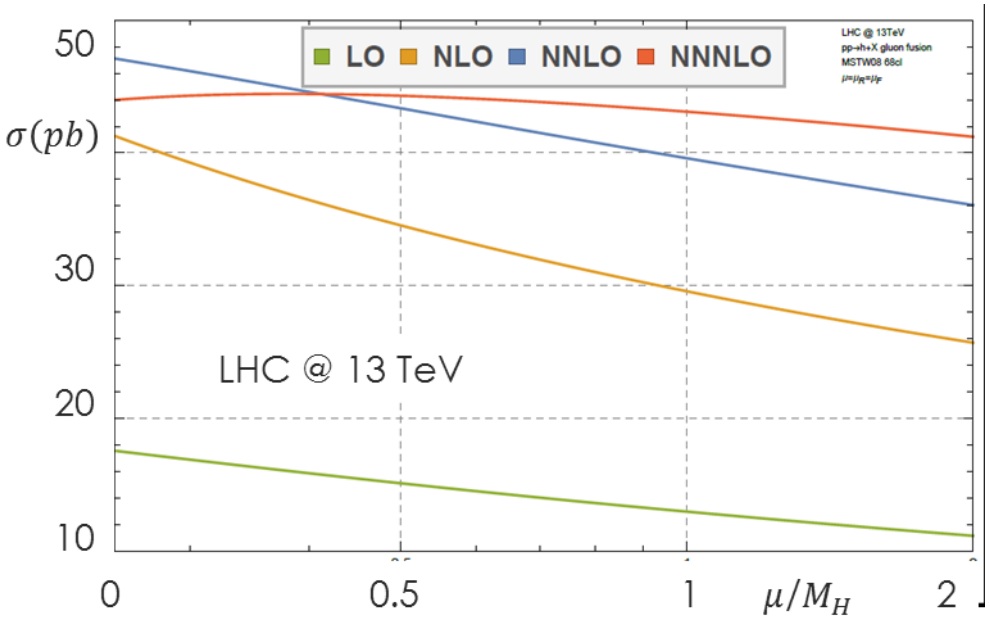

Anastasiou, Duhr, Dulat, Herzog, Mistlberger, 1503.06056

N3LO corrections are of the order of +2.2%. The total scale variation at N3LO is 3%

NNLO for differential distributions

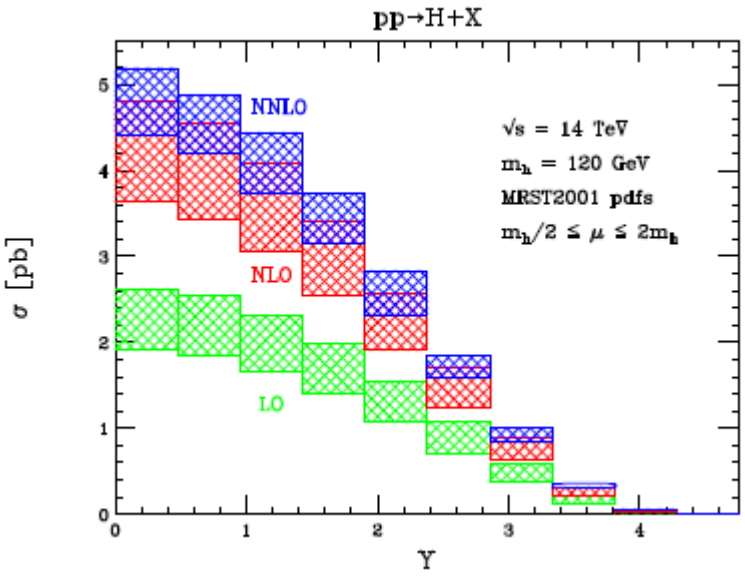

Anastasiou, Melnikov, Petriello, hep-ph/0409088, 0501130

Perturbative QCD loop revolution

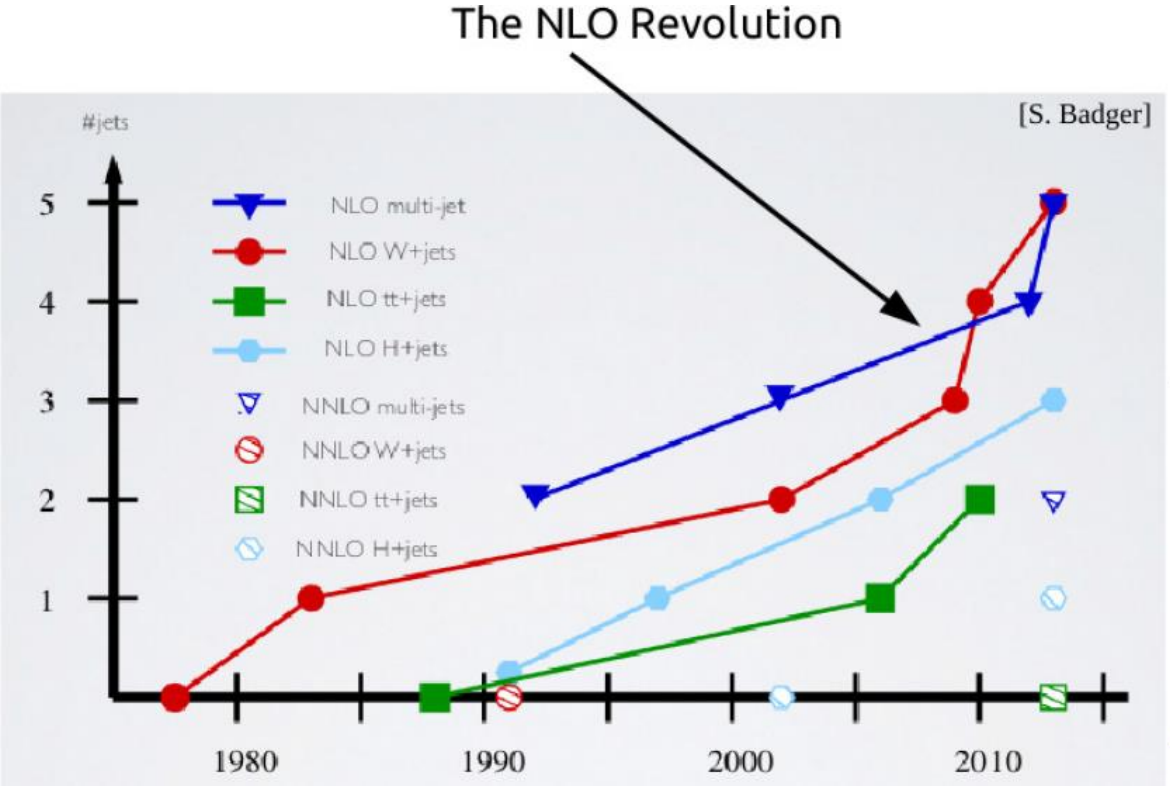

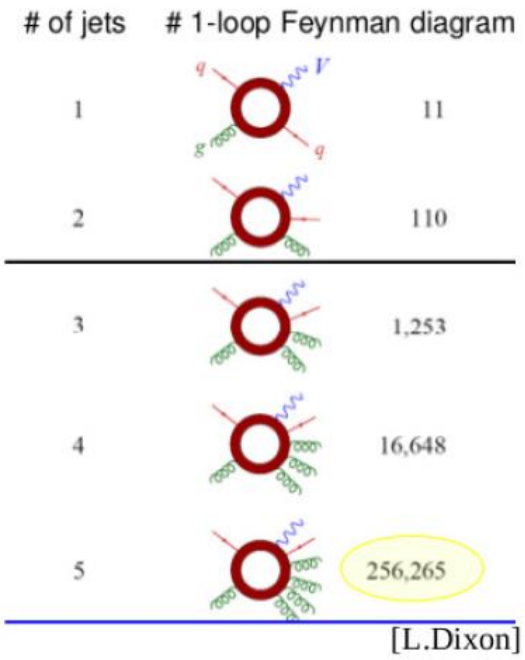

Since 2005, generalized unitarity, sector decomposition, and related methods dramatically advanced the computations of **perturbative** NLO/NNLO/N3LO hard cross sections.

To make use of it, PDF accuracy must keep up

Recent CT14 PDFs

(S. Dulat et al., arXiv:1506.07443)

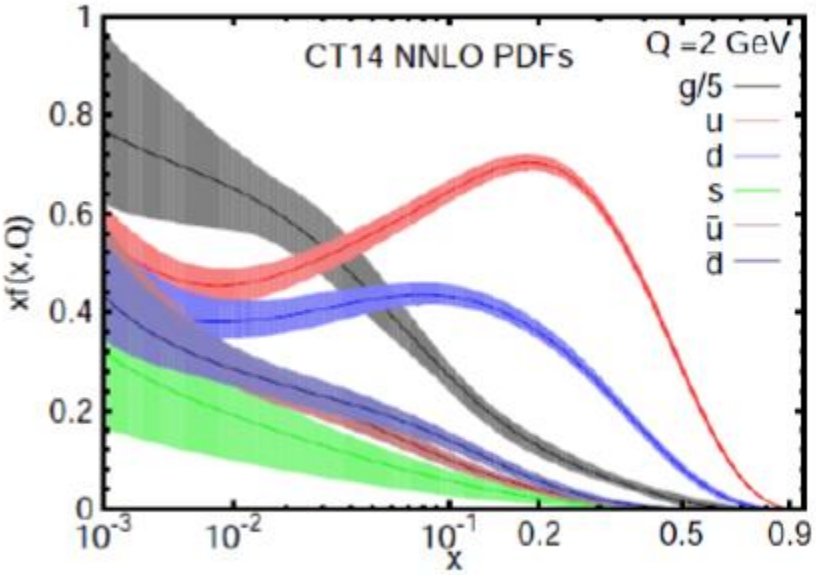

Q= 2 GeV

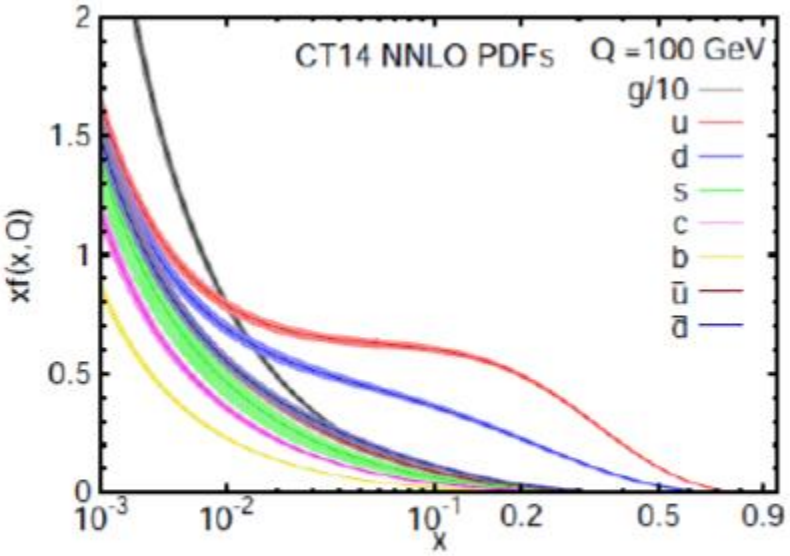

Q= 100 GeV

Phenomenological parametrizations of PDFs are provided with estimated uncertainties of multiple origins (**uncertainties of measurement, theoretical model, parametrization form, statistical analysis**, …)

The shape of PDFs is optimized w.r.t. hundreds of **nuisance parameters**

Recent CT14 PDFs

(S. Dulat et al., arXiv:1506.07443)

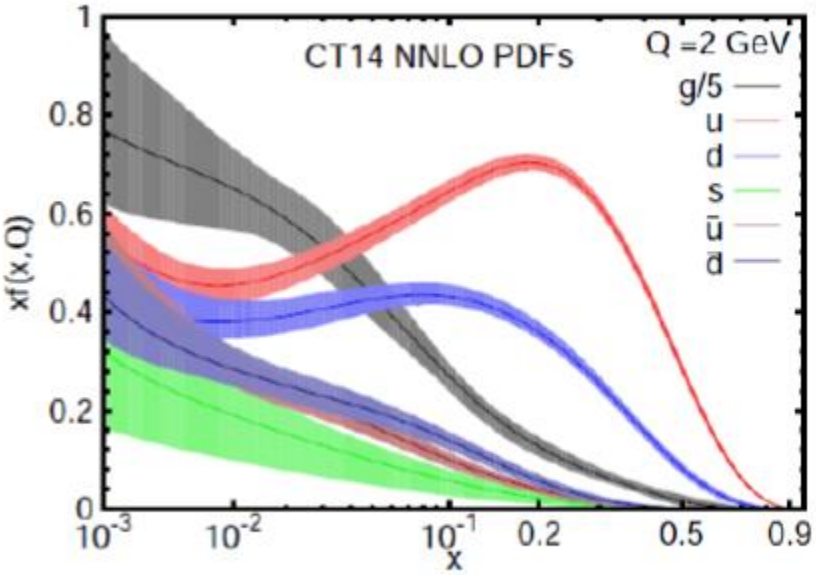

Q= 2 GeV

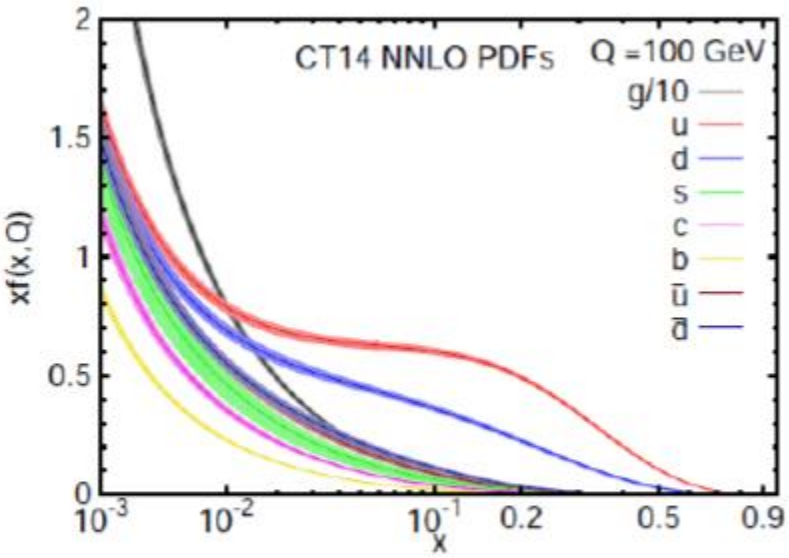

Q= 100 GeV

Accuracy of PDFs is increased by advancing in multiple domains, not only by including perturbative higher orders

"Terribly complex" PDF fits

Great progress to NNLO accuracy, great opportunities

Status of the PDFs in spring 2016

1. General-purpose NNLO PDFs

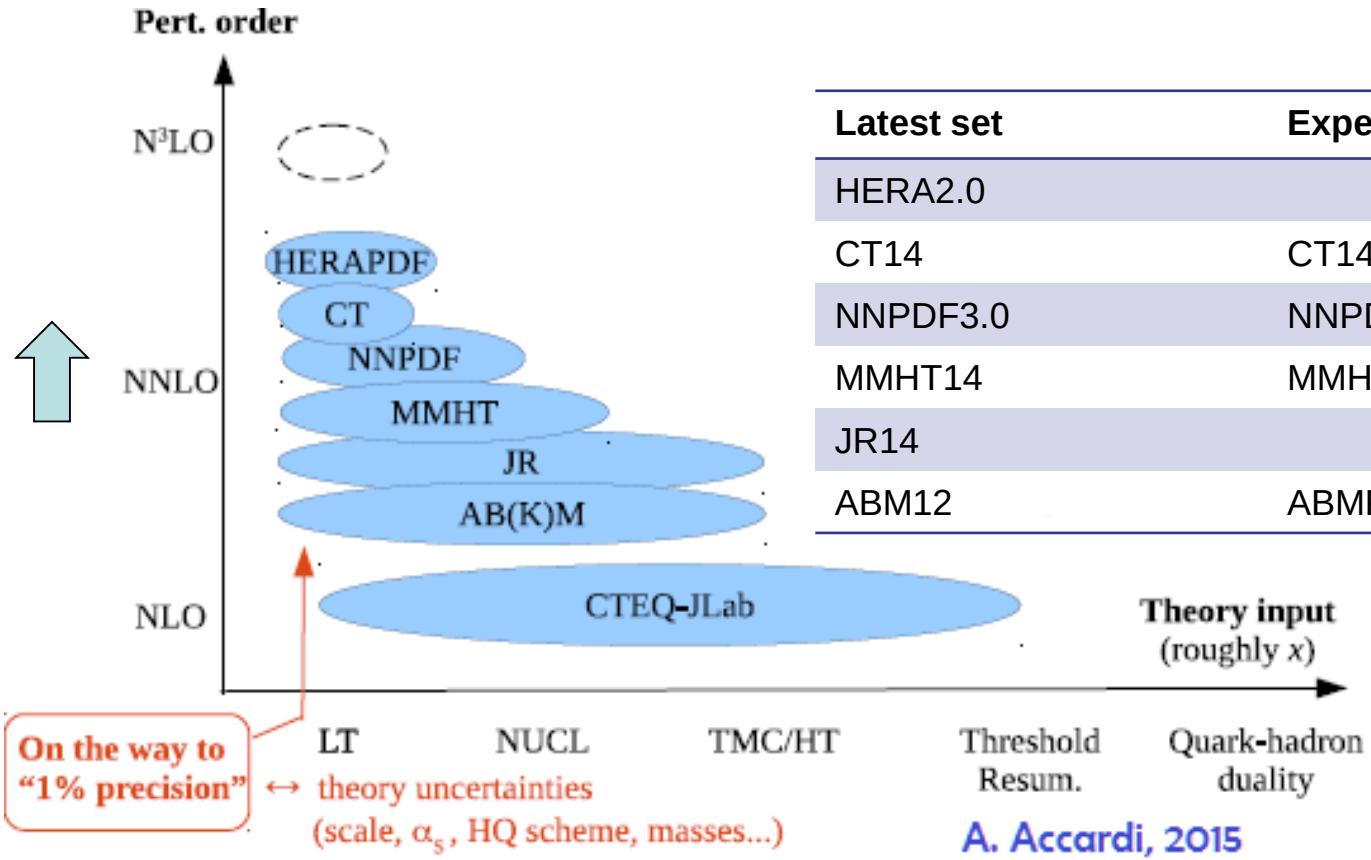

Latest set	Expected updates
HERA2.0	
CT14	CT14HERA2
NNPDF3.0	NNPDF3.1
MMHT14	MMHT+HERA2
JR14	
ABM12	ABMP16

For general-purpose **nucleon** PDFs, the goal is to determine very precise parametrizations for PQCD calculations up to (N)(N)NLO in α_s. The focus is on the high-Q data that is not sensitive to higher twists, small-x, nuclear, and target mass corrections

1. General-purpose NNLO PDFs

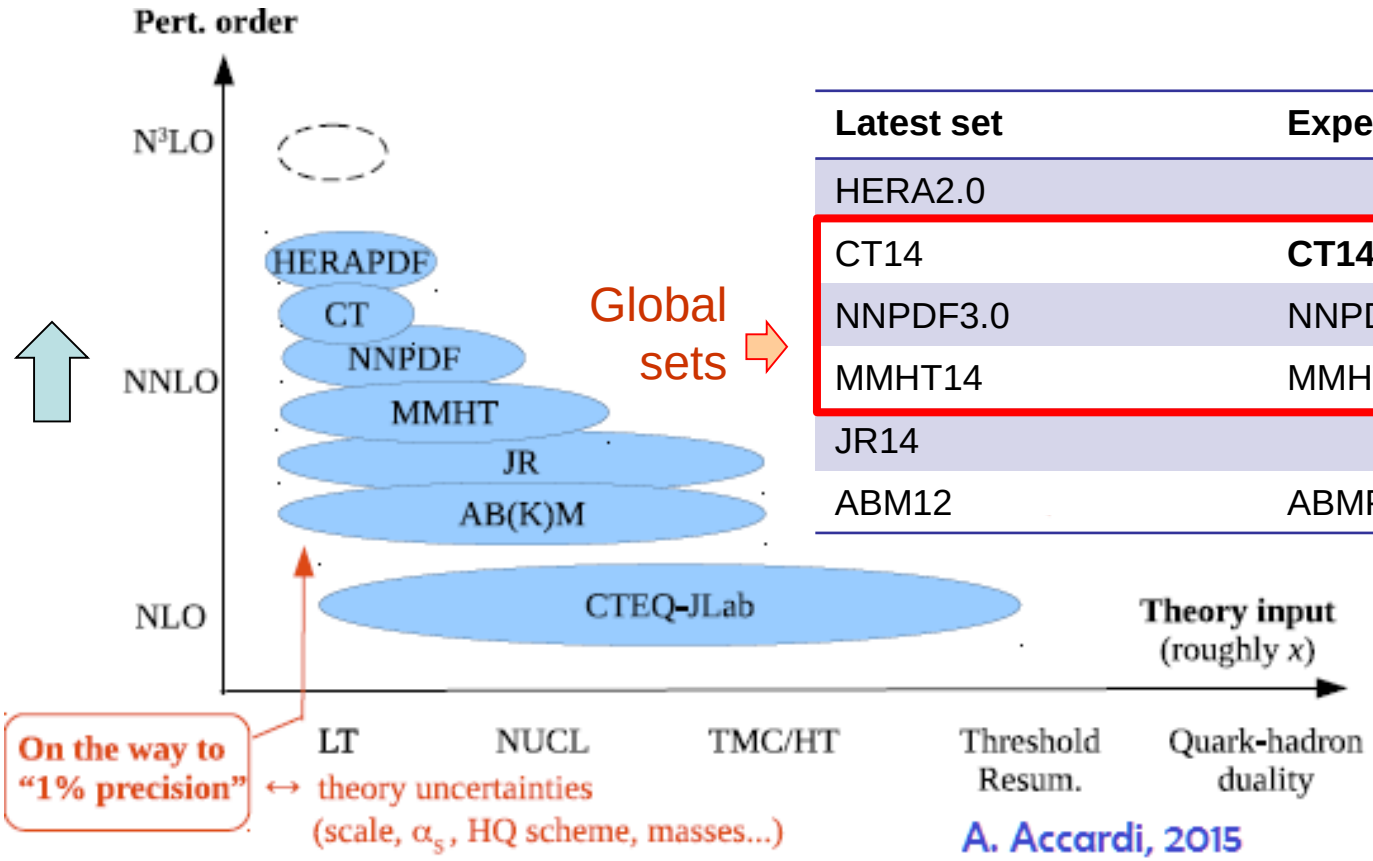

Latest set	Expected updates
HERA2.0	
CT14	**CT14HERA2**
NNPDF3.0	NNPDF3.1
MMHT14	MMHT+HERA2
JR14	
ABM12	ABMP16

2016 updates include new combined HERA1+2 data and 8 TeV LHC data

Expect mild changes in the PDFs and uncertainties

Map of experiments as a function of x and Q

For nucleon PDFs, experimental measurements are selected so as to reduce dependence on theoretical input beyond the leading power in perturbative QCD

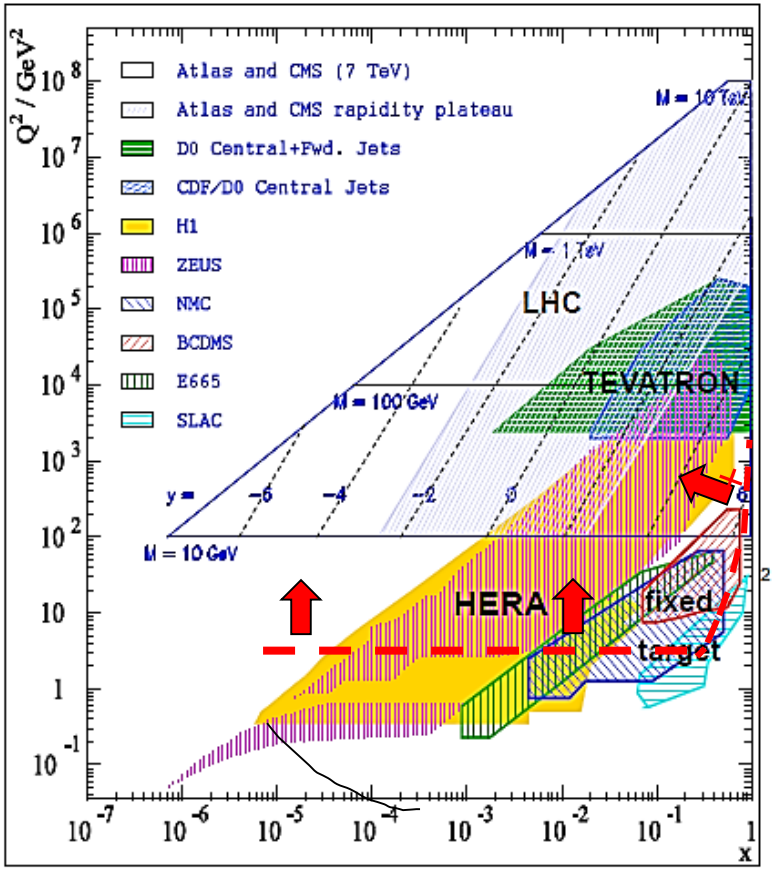

CT14:

only DIS data with $Q^2 > 4\ GeV^2$, $W^2 > 12.25\ GeV^2$ (above the red line) are accepted to ensure stable perturbative predictions

Include LHC W asymmetry and jet production data

Still using data from DIS and DY on **nuclear targets. CT14H2** does not use NMC DIS **on deuteron,** will be replaced by comparable future LHC/Tevatron measurements on **the proton**

Experiments in the CT14 analysis

33 experiments; χ^2/N_{pt} = 3252/2947 =1.10

Red arrows indicate new data sets

Experimental data set		N_{pt}	χ^2_e/N_{pt}
BCDMS F_2^p			
BCDMS F_2^d			
NMC F_2^d/F_2^p	[14]	123	1.08
NMC σ^p_{red}	[14]	201	1.85
CDHSW F_2^p	[15]	85	0.85
CDHSW F_3^p	[15]	96	0.83
CCFR F_2^p	[16]	69	1.02
CCFR xF_3^p	[17]	86	0.36
NuTeV $\nu\mu\mu$ SIDIS	[18]	38	0.62
NuTeV $\bar{\nu}\mu\mu$ SIDIS	[18]	33	1.18
CCFR $\nu\mu\mu$ SIDIS	[19]	40	0.72
CCFR $\bar{\nu}\mu\mu$ SIDIS	[19]	38	0.53
H1 σ_r^b	[20]	10	0.68
HERA charm production		47	1.26
HERA1 Combined NC and CC DIS	[22]	579	1.02
H1 F_L	[23]	9	1.92

Experimental data set		N_{pt}	χ^2_e/N_{pt}
	[24]	119	0.98
	[25]	15	0.87
E866 Drell-Yan process	[25]	184	1.37
CDF Run-1 electron A_{ch}	[26]	11	0.81
CDF Run-2 electron A_{ch}	[27]	11	1.24
D0 Run-2 muon A_{ch}	[29]	9	0.92
LHCb 7 TeV 35 pb^{-1} W/Z $d\sigma/dy_\ell$		14	0.7
LHCb 7 TeV 35 pb^{-1} A_{ch}, $p_{T\ell} > 20$ GeV		5	1.19
D0 Run 2 Z rapidity	[32]	28	0.59
CDF Run 2 Z rapidity	[33]	29	1.64
CMS 7 TeV 4.7 fb^{-1}, muon A_{ch}		11	0.8
CMS 7 TeV 840 pb^{-1}, electron A_{ch}		11	0.87
ATLAS 7 TeV 35 pb^{-1} W/Z cross sections and A_{ch}		41	1.11
D0 Run-2 electron A_{ch} ($9.7 fb^{-1}$)		13	1.79
CDF Run-2 inclusive jet production	[40]	72	1.45
D0 Run-2 inclusive jet production	[41]	110	1.09
ATLAS 7 TeV 35 pb^{-1} incl. jet production		90	0.55
CMS 7 TeV 5 fb^{-1} incl. jet production		133	1.33

Compare CT14 and CT10 quark PDFs

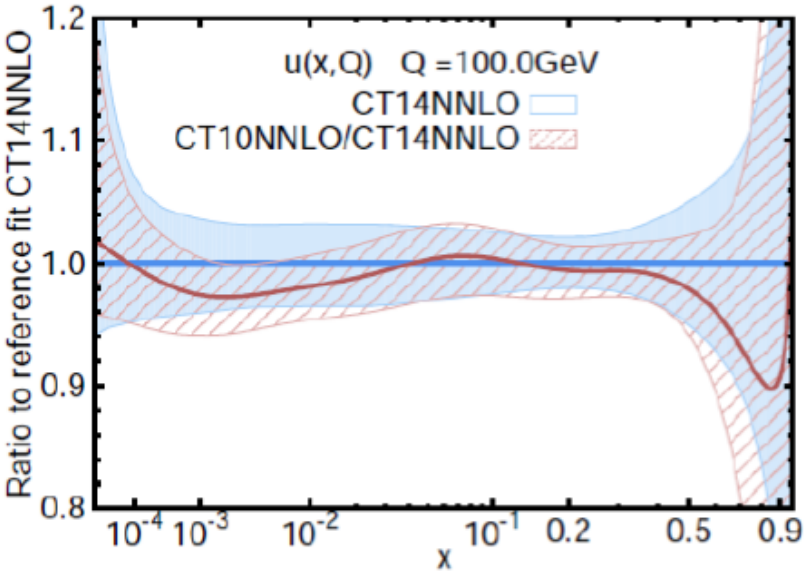

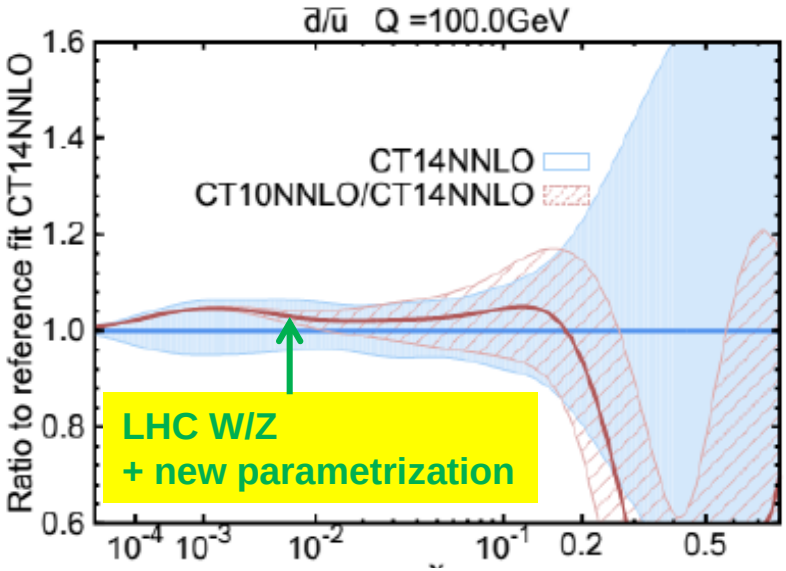

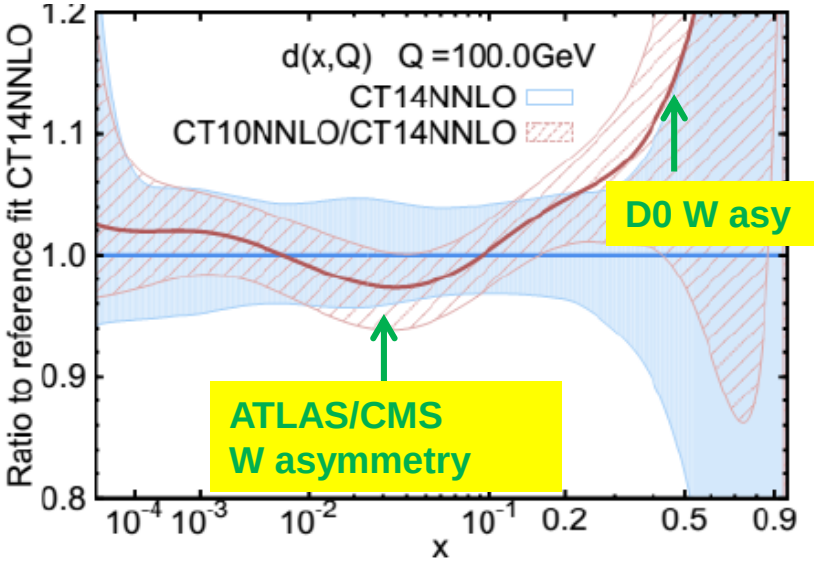

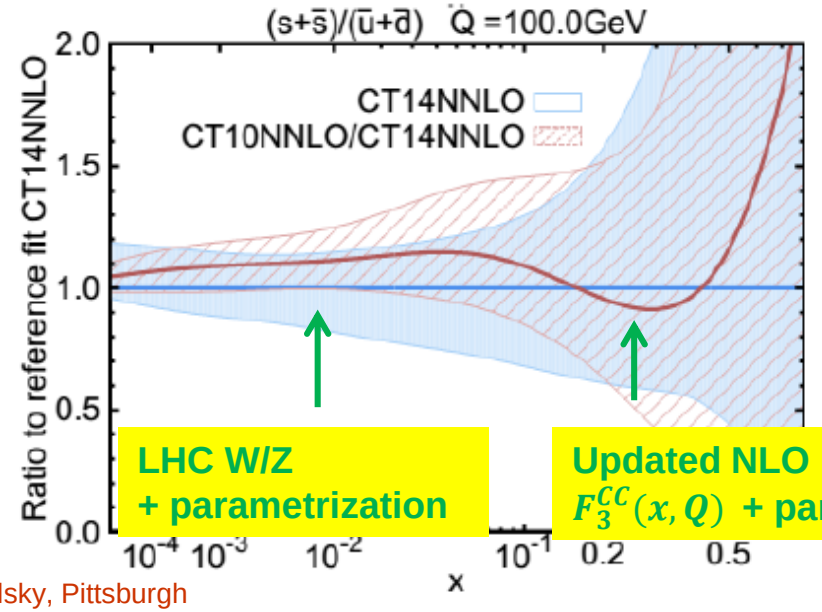

The ratios of W^+ to W^- and $(W^+ + W^-)$ to Z cross sections CT14HERA2 vs. CT14

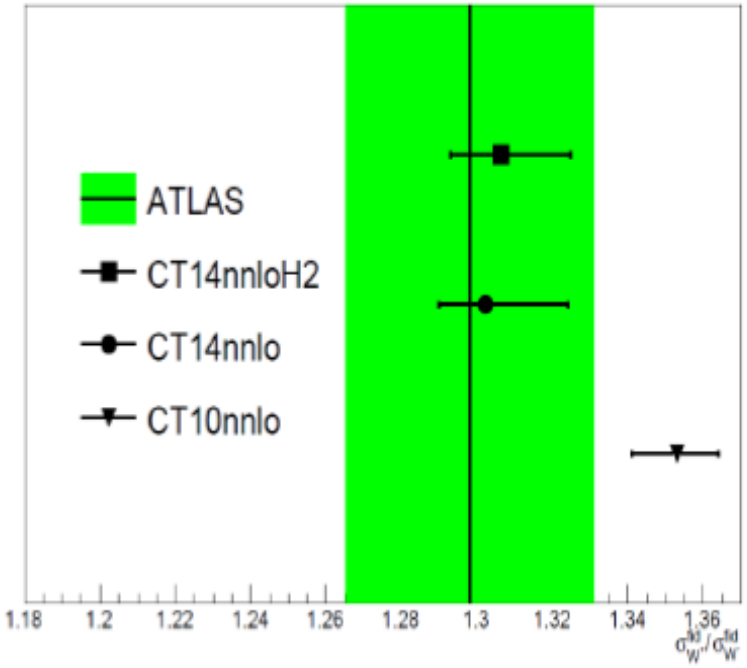

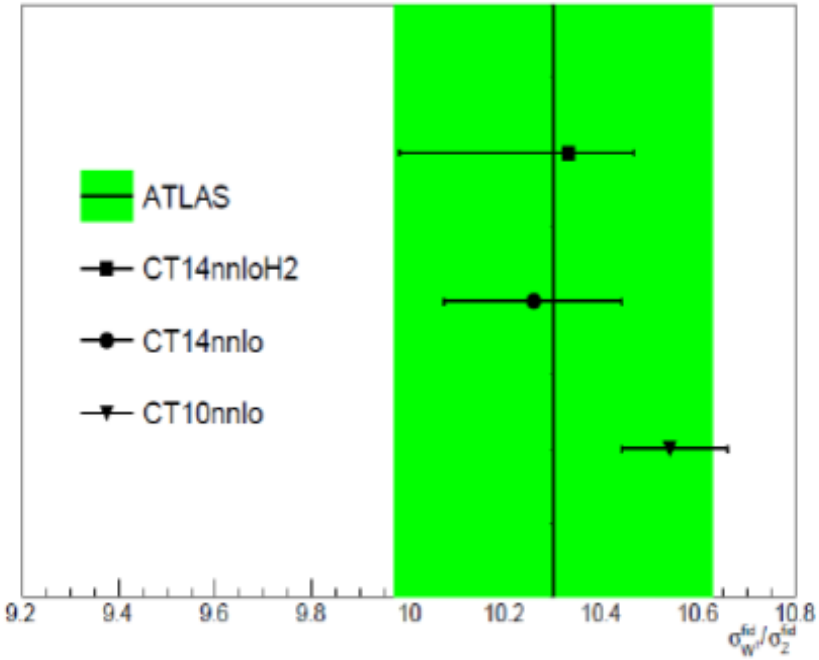

$p_T^l > 25\ GeV\ , \quad |\eta_l| < 2.5\ , \quad 66 < m_{ll} < 116\ GeV$

$p_T^l > 25\ GeV\ , \quad p_T^\nu > 25\ GeV\ , \quad |\eta_l| < 2.5\ , \quad m_T > 50\ GeV$

PRELIMINARY

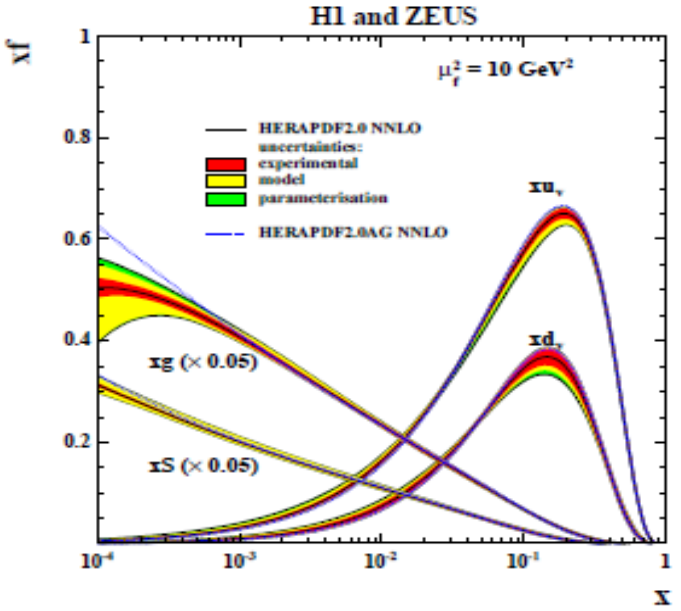

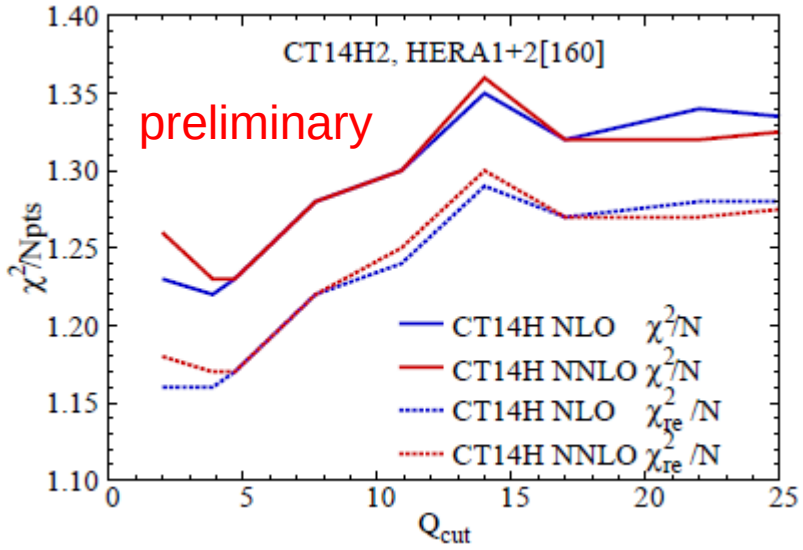

χ^2/N_{pts} with (top) and without (bottom) penalty for syst. shifts

The combined HERA1+2 data are included in HERA2.0, **CT14HERA2**, MMHT, and NNPDF3.1 analyses

$\chi^2/d.o.f. \sim 1.2$ for HERA1+2 tends to be elevated across all analyses, compared to $\chi^2/d.o.f. < 1.1$ for combined HERA1 data

⇒ This tension may arise from several sources

- Higher-twist corrections to $F_L(x, Q)$
- Small-x/saturation
- Experimental systematics (?)

The impact on global PDFs is mild, changes in PDFs do not exceed uncertainties

CT14HERA2: effect of increasing the statistical weight of HERAI+II data from w=1 to w=6

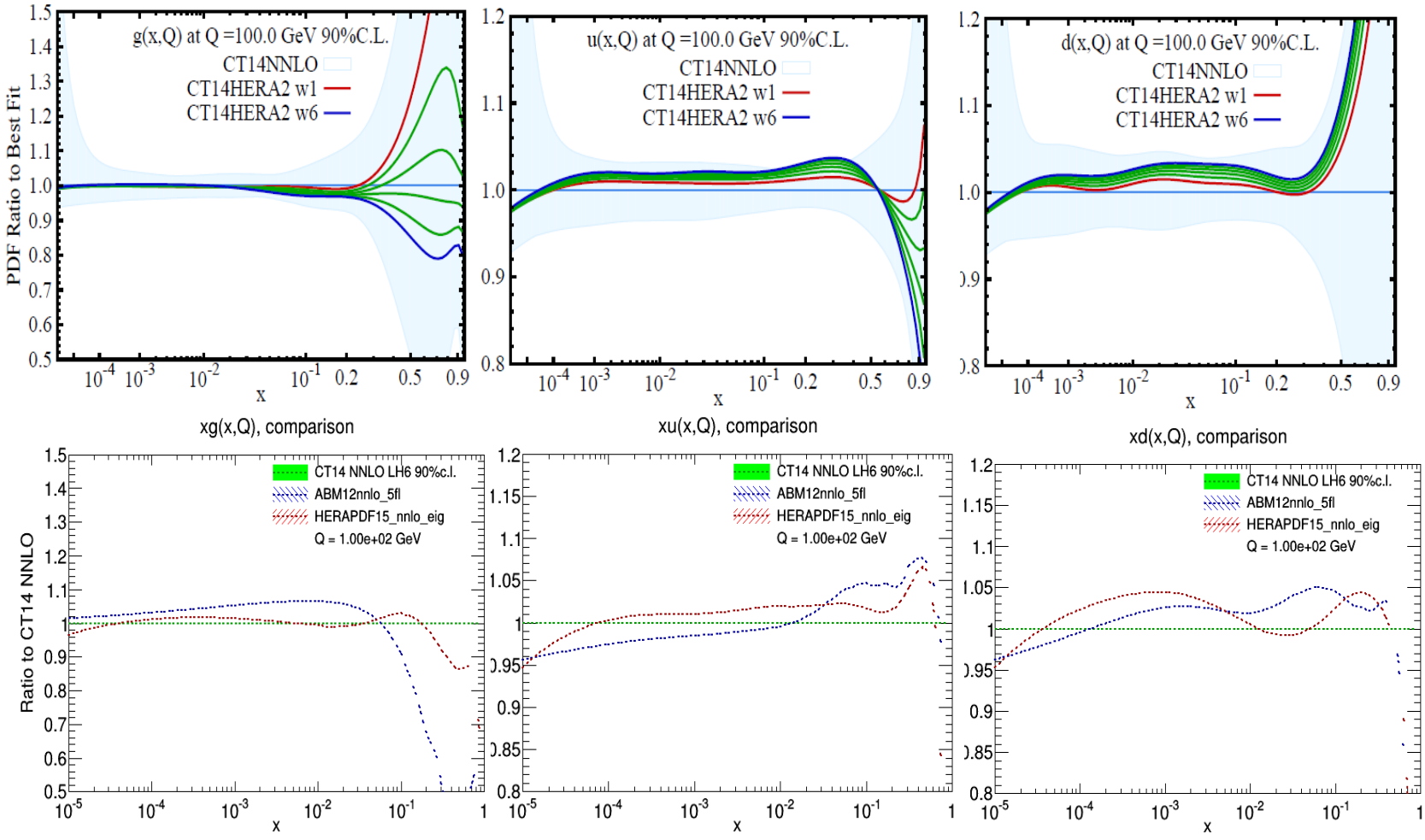

With $w = 6$, CT14HERA2 PDFs for g, u, and d are more similar to HERA2.0, not to ABM12 in a different theory framework with $\alpha_s = 0.113$

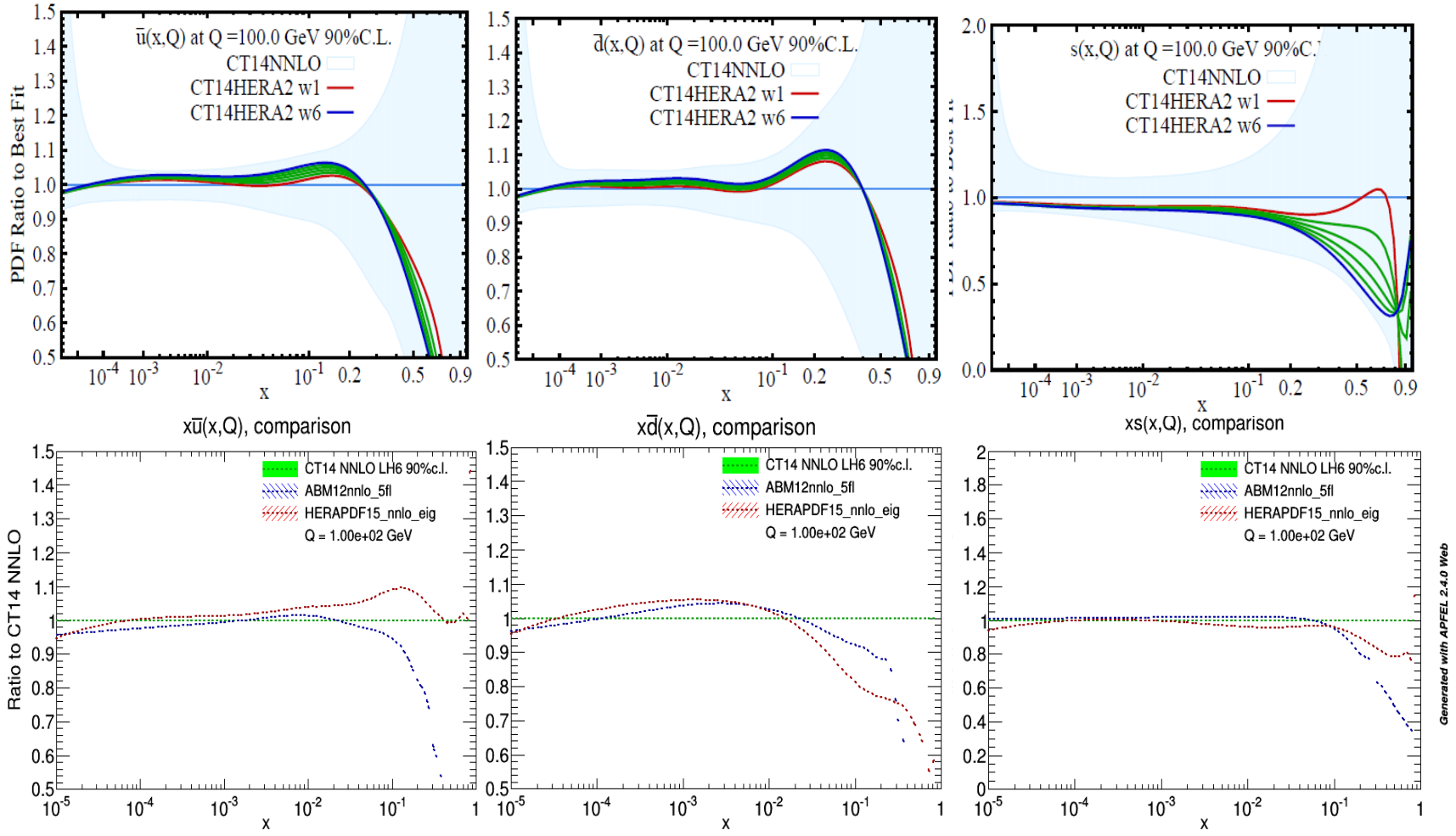

For sea PDFs, similarity is less pronounced (not as sensitive to HERA DIS)

2. Specialized PDFs at NLO and NNLO

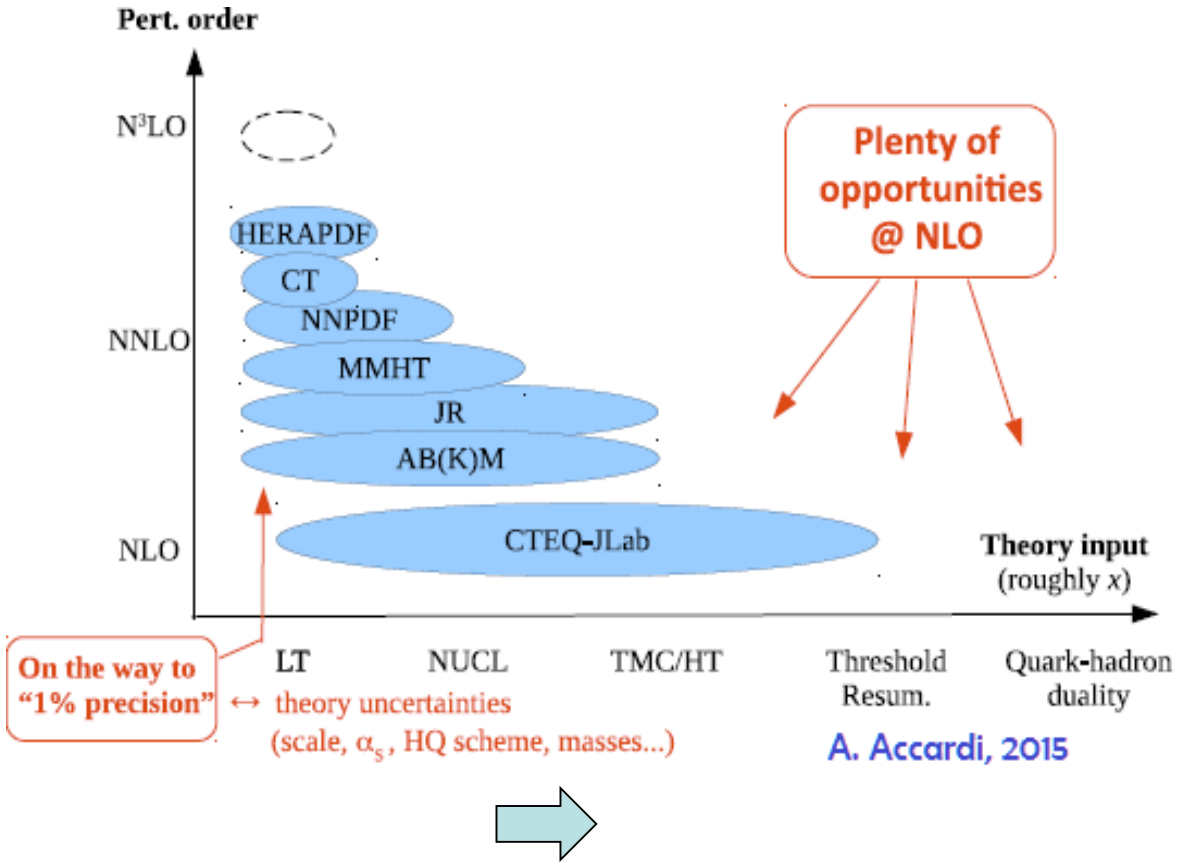

Are obtained under special assumptions or for special goals. May or may not be suitable for general physics

1. **CJ15:** NLO PDFs with large-x/low Q DIS data
2. **Most groups:** PDFs with up to 3, 4 active flavors
3. **CT, NNPDF, MSTW:** QCD+QED PDFs
4. **CT, NNPDF:** PDFs with intrinsic charm
5. **NNPDF:** PDFs for threshold resummation
6. **…**

See backup slides

2012→2015: Agreement between global NNLO PDFs greatly improved

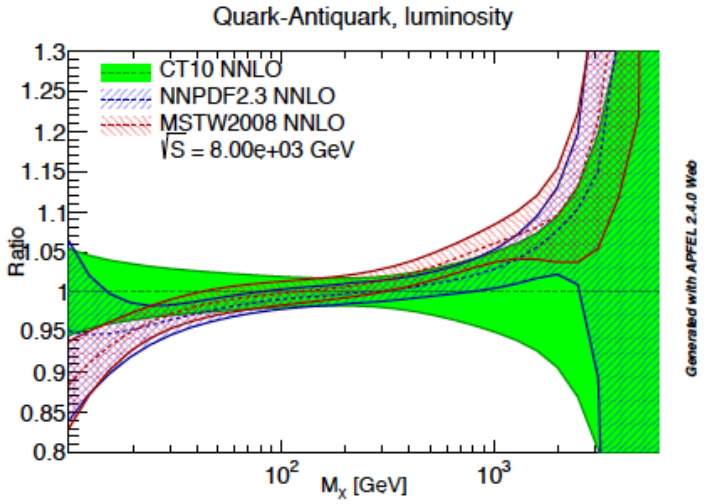

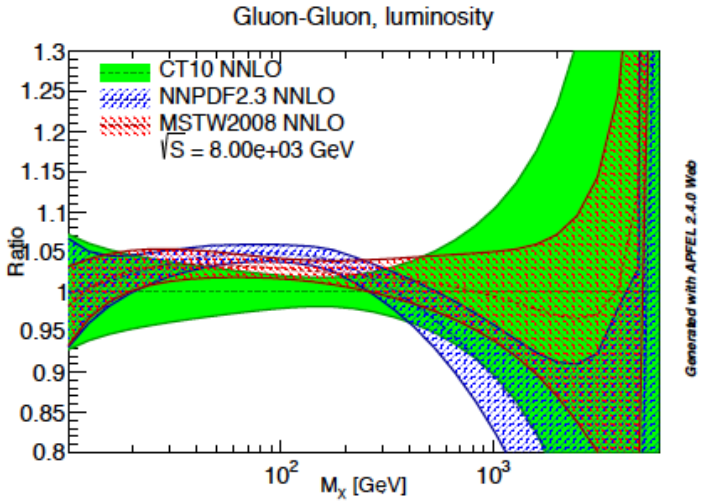

Figure 1: Comparison of the $q\bar{q}$ (left) and gg (right) PDF luminosities at the LHC 8 TeV for CT10, MSTW2008 and NNPDF2.3. Results are shown normalized to the central value of CT10.

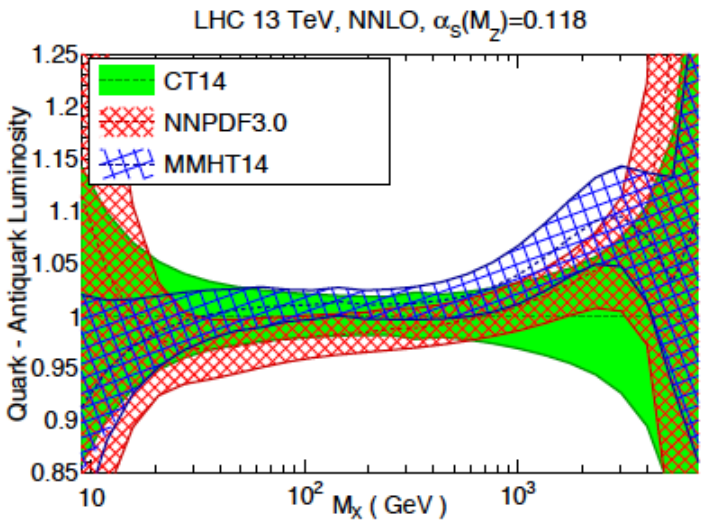

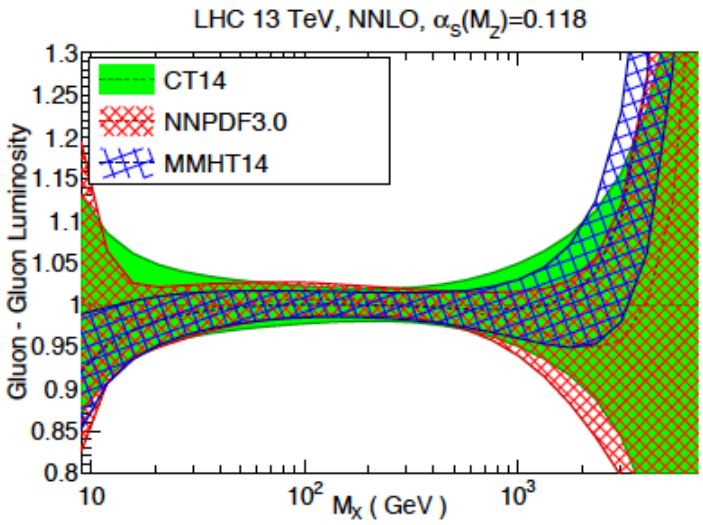

Note in particular the changes in the gg luminosity, especially important in the Higgs mass region

LHC data has been added for all 3 new PDFs, but most changes are due to benchmarking of formalisms

Other new sets published as well

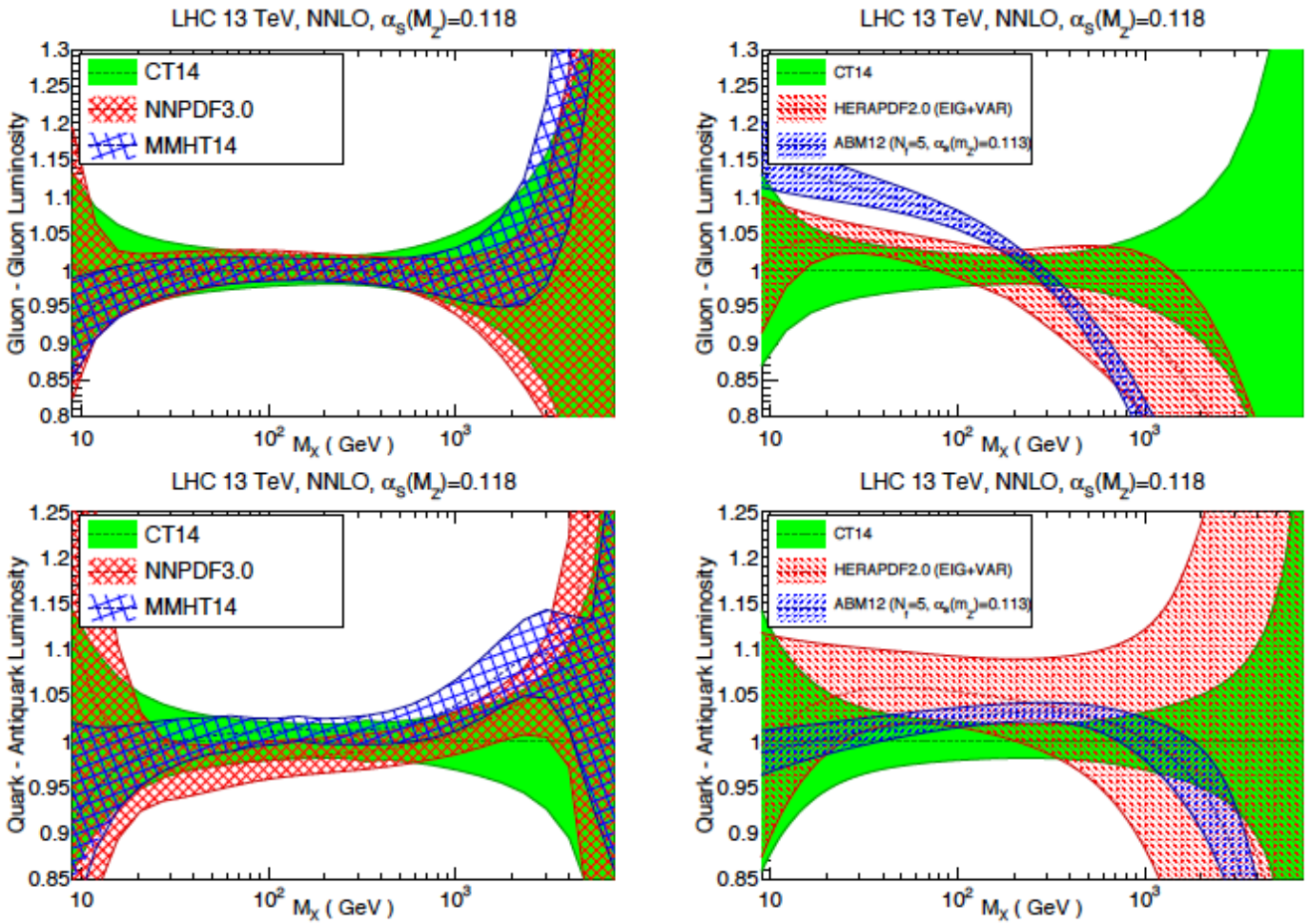

behavior for HERAPDF2.0 and ABM12 somewhat different

HERAPDF2.0 uncertainties tend to be larger

Figure 5: Comparison of the gluon-gluon (upper plots) and quark-antiquark (lower plots) PDF luminosities from the CT14, MMHT14 and NNNPDF3.0 NNLO sets (left plots) and from the NNPDF3.0, ABM12 and HERAPDF2.0 NNLO sets (right plots), for a center-of-mass energy of 13 TeV, as a function of the invariant mass of the final state M_X.

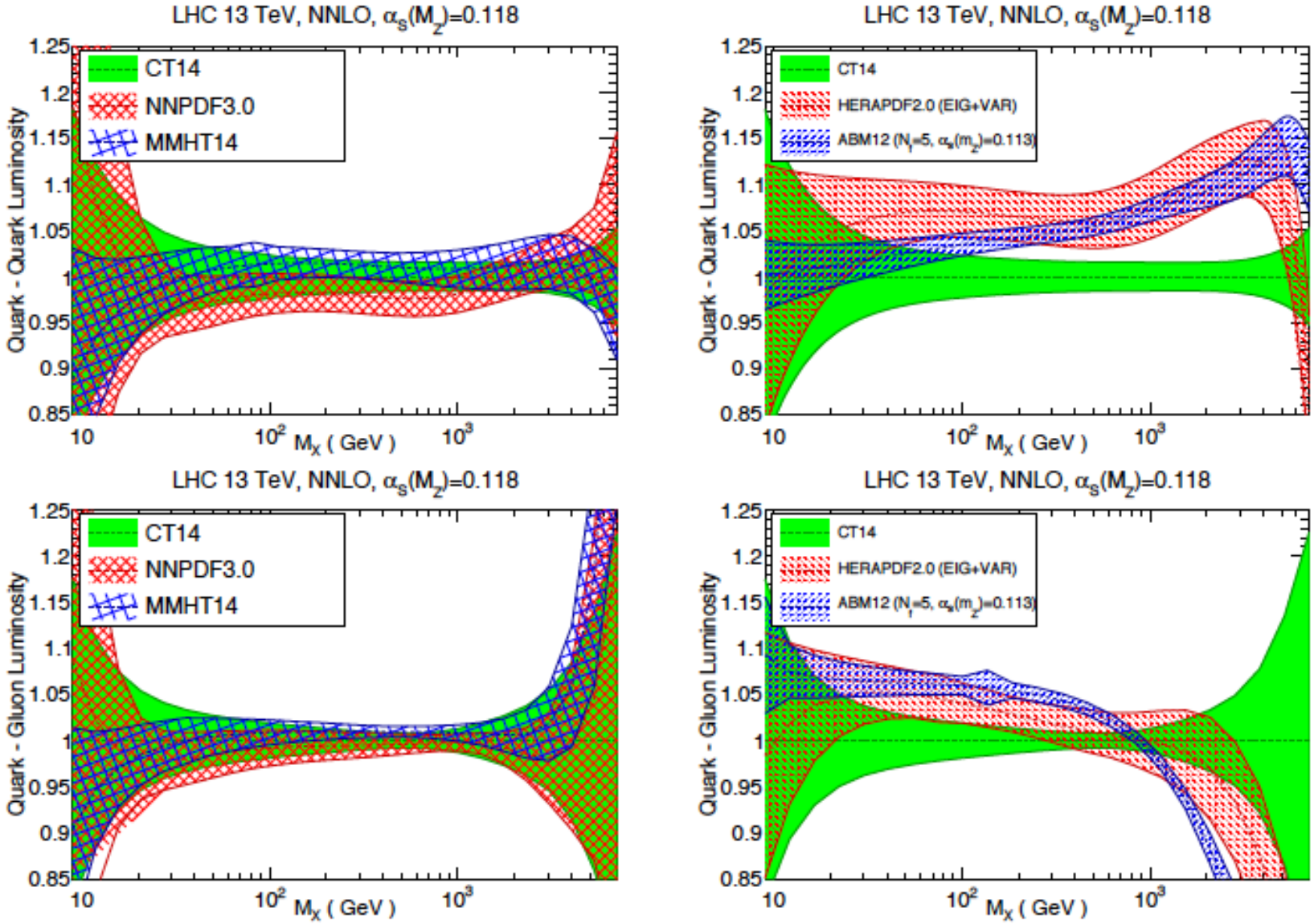

Figure 6: Same as Fig. 5 for the quark-quark (upper plots) and the quark-gluon (lower plots) PDF luminosities.

Why global NNLO PDFs are in better agreement now than ever

To start, various NNLO calculations have reduced dependence on renormalization, factorization, and auxiliary mass scales than at NLO

Since 2012, PDF analysis groups carried out a series of benchmarking exercises for key processes of DIS and jet production in PDF fits

Methodologies of all groups were cross-validated and improved.

Theoretical accuracy

A variety of comparisons was accomplished to benchmark NNLO theoretical calculations for key scattering processes

1.J. Gao et al., MEKS: a program for computation of inclusive jet cross sections at hadron colliders , arXiv:1207.0513

2. R. Ball et al., Parton Distribution benchmarking with LHC data, arXiv:1211.5142

3. S. Alekhin et al., ABM11 PDFs and the cross section benchmarks in NNLO, arXiv:1302.1516; The ABM parton distributions tuned to LHC data; arXiv:1310.3059

4. A.Cooper-Sarkar et al., PDF dependence of the Higgs production cross section in gluon fusion from HERA data, 2013 Les Houches Proceedings, arXiv:1405.1067, p. 37

5. S. Forte and J. Rojo, Dataset sensitivity of the gg->H cross-section in the NNPDF analysis, arXiv:1405.1067, p. 56

Verifying statistical methods

Parametric/Hessian methodology (CT, MMHT) and **nonparametric/Monte-Carlo methodology** (NNPDF) result in comparable global fits and PDF uncertainties

Advanced PDF parametrizations are employed by CT and MMHT for efficient, minimally biased, extraction of PDFs from global data

Hessian PDFs can be converted into MC PDFs, and back

CT14 replicas Hou. Study of asymmetric uncertaities.

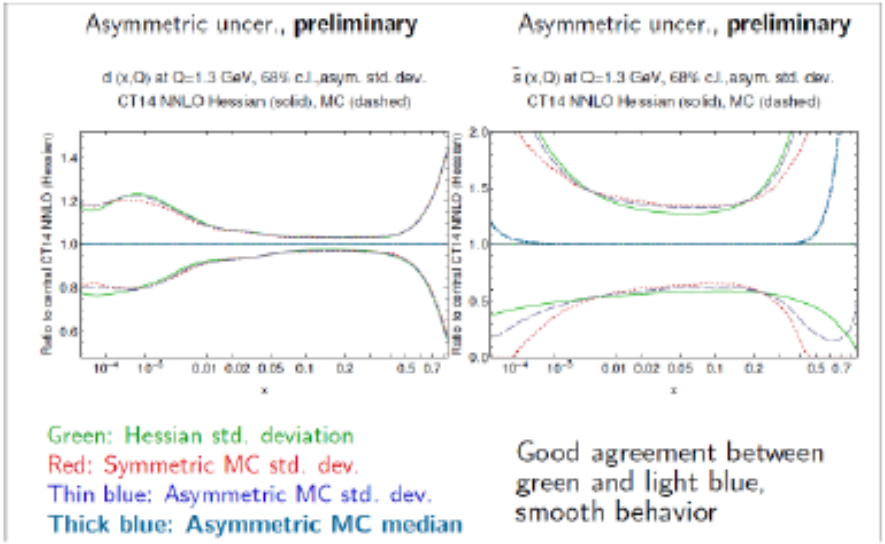

Also plot of χ^2 distribution for 1000 replicas with 28 eigenvectors and tolerance $\sim$ 40 for one sigma. Extremely similar to NNPDF from completely different approach.

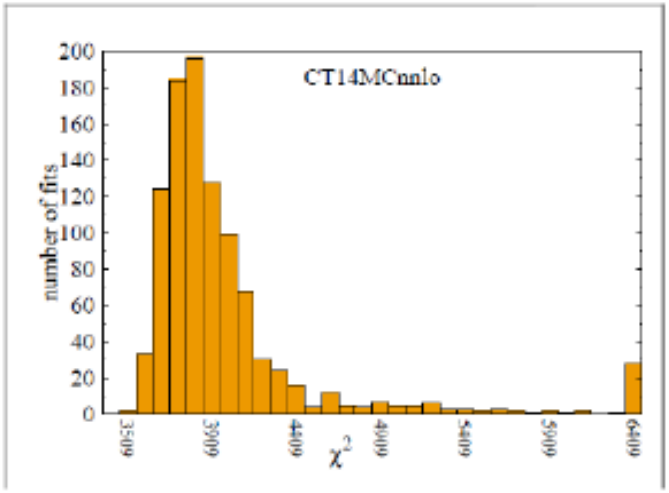

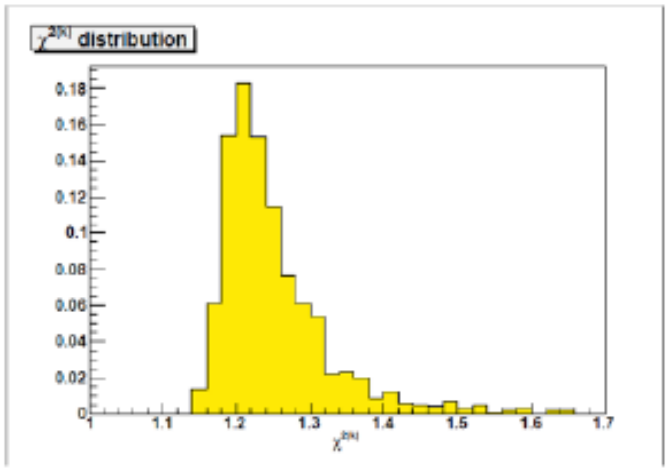

Example: $gg \to H^0_{SM}$ at the LHC

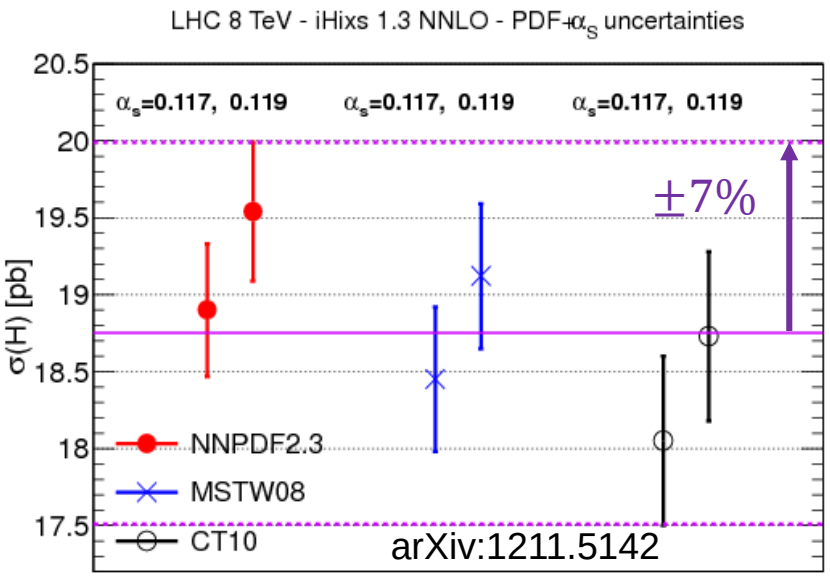

	CT14	MMHT2014	NNPDF3.0
8 TeV	18.66 pb -2.2% +2.0%	18.65 pb -1.9% +1.4%	18.77 pb -1.8% +1.8%
13 TeV	42.68 pb -2.4% +2.0%	42.70 pb -1.8% +1.3%	42.97 pb -1.9% +1.9%

J.Huston, PDF4LHC, April 2015

For example, δ_{PDF} on Higgs cross sections based on 3 **latest** global fits has reduced from 7% to within 3%, i.e., the PDF uncertainty is now of order of N3LO QCD scale uncertainty

This improvement is due to benchmarking of general-mass factorization schemes; but can there be hidden sources of uncertainties on $\sigma(gg \to H)$, e.g., associated with massive charm DIS contributions, cf. arXiv:1603.08906?

No. Uncertainty on $\sigma(gg \to H)$ due to $m_c(m_c)$ is <2-3%

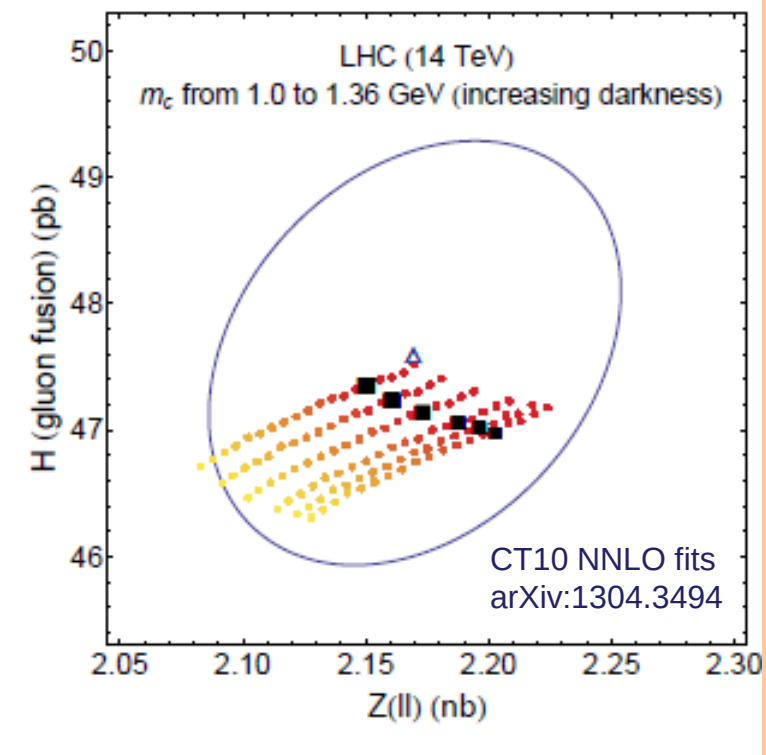

σ_{tot} for $m_c(m_c) = 1 - 1.36$ GeV and matching parameter λ varied independently, $Q_0 = 1$ GeV. Black boxes are for $m_c(m_c) = 1.28$ GeV (close to world average), for the explored λ. The error ellipse is for nominal 90% C.L. @ $Q_0 = 1.3$ GeV.

GM-VFN schemes agree well at NNLO because of perturbative convergence, not because of m_c tuning

Intrinsic charm only reduces correlated dependence on m_c, Q_0, and matching (NNPDF)

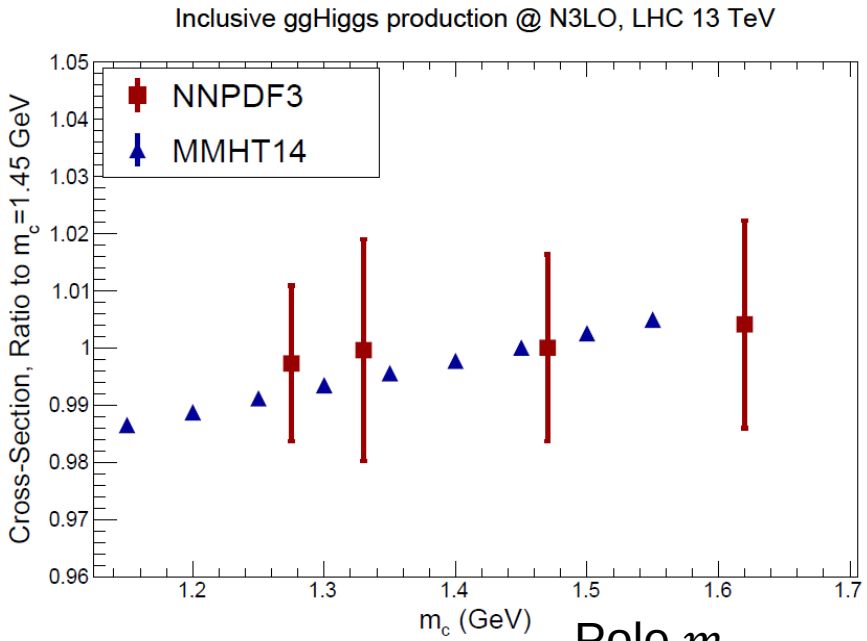

Pole m_c

Estimating the PDF+α_s uncertainty in practical applications

Given numerous PDF sets, what is the PDF uncertainty in my analysis?

$pp \to t\bar{t}X$

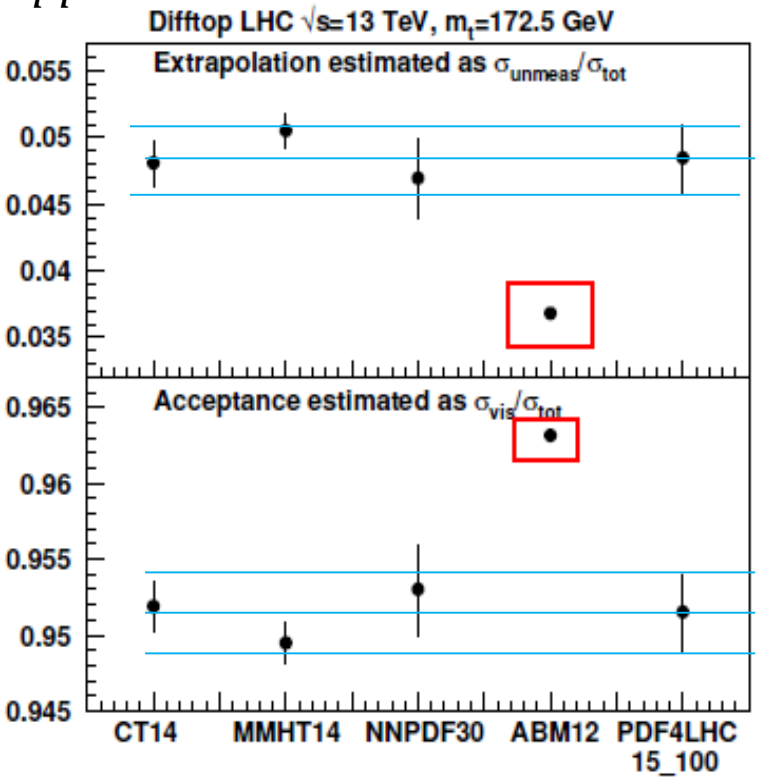

Figure: K. Lipka 1603.08906

The procedure for computing the PDF uncertainty must vary depending on the goals. The options may include

a) Using one individual set out of several similar ones (e.g., CT, MMHT, or NNPDF)

b) Using an envelope of all sets, including the outlier sets

c) 2015 recommendation by the PDF4LHC working group (arXiv:1510.03865)**:**

1. Several procedures spelled out for computation of PDF uncertainties, depending on the context
2. Estimation of PDF uncertainties is streamlined in many cases by using combined PDF4LHC15 sets based on CT14, MMHT14, and NNPDF3.0

Why PDF4LHC recommendation is necessary

Estimates of PDF uncertainties may vary drastically depending on the method.

An overly conservative estimate greatly reduces sensitivity to BSM physics.

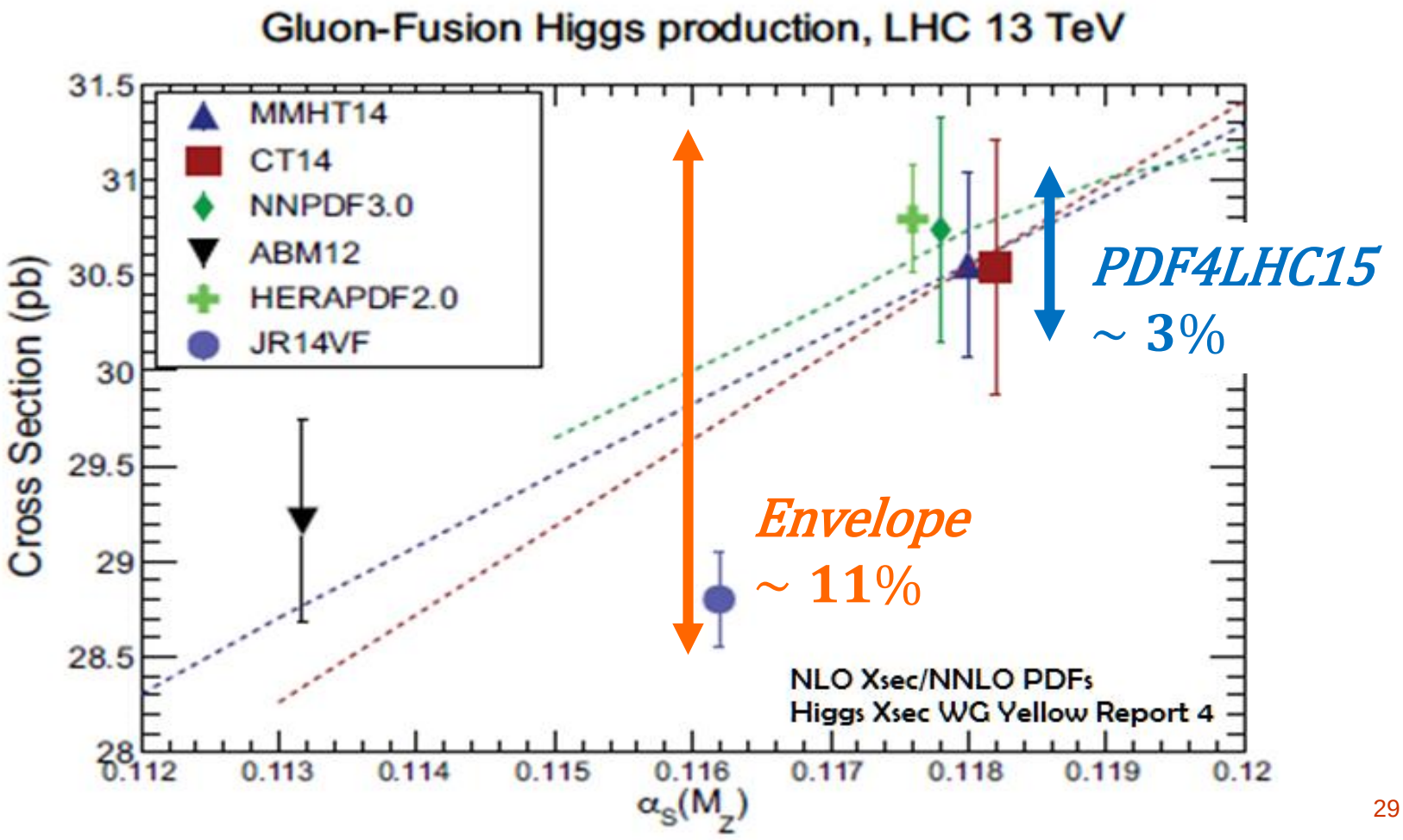

Why PDF4LHC recommendation is needed

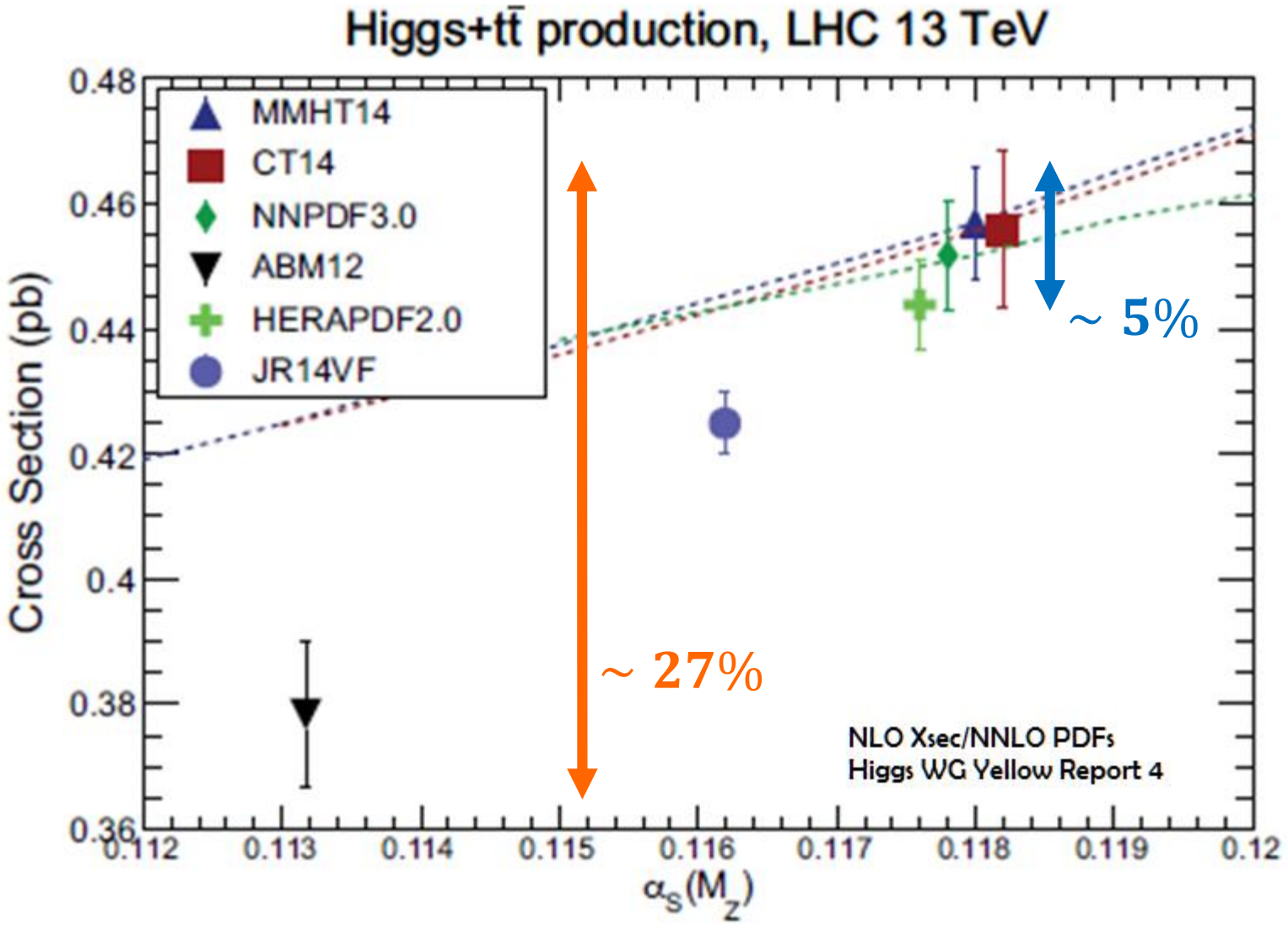

OUTP-15-17P
SMU-HEP-15-12
TIF-UNIMI-2015-14
LCTS/2015-27

PDF4LHC recommendations for LHC Run II

Jon Butterworth[1], Stefano Carrazza[2], Amanda Cooper-Sarkar[3], Albert De Roeck[4,5], Joël Feltesse[6], Stefano Forte[2], Jun Gao[7], Sasha Glazov[8], Joey Huston[9], Zahari Kassabov[2,10], Ronan McNulty[11], Andreas Morsch[4], Pavel Nadolsky[12], Voica Radescu[13], Juan Rojo[14] and Robert Thorne[1].

[1] *Department of Physics and Astronomy, University College London, Gower Street, London WC1E 6BT, UK.*
[2] *TIF Lab, Dipartimento di Fisica, Università di Milano and INFN, Sezione di Milano, Via Celoria 16, I-20133 Milano, Italy*
[3] *Particle Physics, Department of Physics, University of Oxford, 1 Keble Road, Oxford OX1 3NP, UK.*
[4] *PH Department, CERN, CH-1211 Geneva 23, Switzerland*
[5] *Antwerp University, B2610 Wilrijk, Belgium*
[6] *CEA, DSM/IRFU, CE-Saclay, Gif-sur-Yvette, France*
[7] *High Energy Physics Division, Argonne National Laboratory, Argonne, Illinois 60439, U.S.A.*
[8] *Deutsches Elektronen-Synchrotron (DESY), Notkestrasse 85, D-22607 Hambury, Germany.*
[9] *Department of Physics and Astronomy, Michigan State Universi East Lansing, MI 48824 U.S.A.*
[10] *Dipartimento di Fisica, Università di Torino and INFN, Sezione di Via Pietro Giuria 1, I-10125 Torino, Italy*
[11] *School of Physics, University College Dublin Science Centre No UCD Belfeld, Dublin 4, Ireland*
[12] *Department of Physics, Southern Methodist University, Dallas, TX 75275*
[13] *Physikalisches Institut, Universität Heidelberg, Heidelberg, Germ*
[14] *Rudolf Peierls Centre for Theoretical Physics, 1 Keble Road, University of Oxford, OX1 3NP Oxford, UK*

A major revision of the previous PDF4LHC recommendation in arxiv:1101.0538, arXiv:1211.5142

+ 2 follow-up contributions in 2015 Les Houches proceedings

Abstract:

PDF4LHC publication, topics

1. **Review of updates on PDFs from various groups**

NNLO Global PDF sets: CT14, MMHT'14, NNPDF3

PDFs using other methodologies: ABM'12, CJ15, HERAPDF2.0

2. Average PDF sets by PDF4LHC group: PDF4LHC15_30, _100, _MC

Criteria for combination

$\alpha_s(M_Z) = 0.1180 \pm 0.0015$ at 68% c.l.

3. Recommendation on selecting PDF sets for various LHC applications

A. New physics searches

B. Precision tests of SM and PDFs

C. Monte-Carlo simulations

D. Acceptance estimates

Average PDF sets **can** be used **for bulk of applications** in A, C, D

Now on LHAPDF:

NLO, NNLO, varied α_s sets
$N_f = 5$ and 4 (upcoming)

LHAPDF6 grid	Pert order	ErrorType	N_{mem}	$\alpha_s(m_Z^2)$
PDF4LHC15_nnlo_mc	NNLO	replicas	100	0.118
PDF4LHC15_nnlo_100	NNLO	symmhessian	100	0.118
PDF4LHC15_nnlo_30	NNLO	symmhessian	30	0.118
PDF4LHC15_nnlo_mc_pdfas	NNLO	replicas+as	102	mem 0:100 → 0.118 mem 101 → 0.1165 mem 102 → 0.1195
PDF4LHC15_nnlo_100_pdfas	NNLO	symmhessian+as	102	mem 0:100 → 0.118 mem 101 → 0.1165 mem 102 → 0.1195
PDF4LHC15_nnlo_30_pdfas	NNLO	symmhessian+as	32	mem 0:30 → 0.118 mem 31 → 0.1165 mem 32 → 0.1195
PDF4LHC15_nnlo_asvar	NNLO	-	1	mem 0 → 0.1165 mem 1 → 0.1195

Table 5: Summary of the combined NNLO PDF4LHC15 sets with $n_f^{\mathrm{max}} = 5$ that are available from LHAPDF6. The corresponding NLO sets are also available. Members 0 and 1 of PDF4LHC15_nnlo_asvar coincide with members 101 and 102 (31 and 32) of PDF4LHC15_nnlo_mc_pdfas and PDF4LHC15_nnlo_100_pdfas (PDF4LHC15_nnlo_30_pdfas). Recall that in LHAPDF6 there is always a zeroth member, so that the total number of PDF members in a given set is always $N_{\mathrm{mem}} + 1$. See text for more details.

Three main uses of PDFs at the LHC

1. Assessment of the *total uncertainty on a cross section* based on the available knowledge of PDFs, *e.g.*, when computing the cross section for a process that has not been measured yet (such as supersymmetric particle production cross-sections), or for estimating acceptance corrections on a given observable. This is also the case of the measurements that aim to verify overall, but not detailed, consistency with Standard Model expectations, such as when comparing theory with Higgs measurements.

2. Assessment of the accuracy of the *PDF sets themselves* or of related Standard Model parameters, typically done by comparing theoretical predictions using individual PDF sets to the most precise data available.

3. Input to the *Monte Carlo event generators* used to generate large MC samples for LHC data analysis.

For 2), compute cross sections with individual PDF sets.

For 1) or 3), the PDF uncertainty based on the totality of available PDF sets must be estimated. Estimate the combined PDF error using **an average of various PDF sets**.

Follow-up publications
In 2015 Les Houches proceedings

Address questions not covered in the main document of 2015 PDF4LHC recommendation (**arXiv:1510.03865**), and provide illustrations

1. **Phenomenological applications of PDF4LHC distributions**

J. Gao, T.-J. Hou, J. Huston, P. N., B. Wang, K. Xie, …

Physics issues, predictions for typical QCD cross sections

2. On the accuracy and Gaussianity of the PDF4LHC15 combined sets of parton distributions

S.Carrazza, S. Forte, Z. Kassabov, J. Rojo

Comparisons of PDF4LHC ensembles, non-Gaussian effects

Choosing the right PDF set for an LHC application

6.1 Delivery and guidelines

The PDF4LHC15 combined PDFs are based on an underlying Monte Carlo combination of CT14, MMHT14 and NNPDF3.0, denoted by MC900, which is made publicly available in three different reduced delivery forms:

- **PDF4LHC15_mc**: a *Monte Carlo PDF set* with $N_{\rm rep} = 100$ replicas.
- **PDF4LHC15_30**: a *symmetric Hessian PDF set* with $N_{\rm eig} = 30$ eigenvectors.
- **PDF4LHC15_100**: a *symmetric Hessian PDF set* with $N_{\rm eig} = 100$ eigenvectors.

In the three cases, combined sets are available at NLO and at NNLO, for the central value of $\alpha_s(m_Z^2) = 0.118$. In addition, we provide additional sets which contain the central values for $\alpha_s(m_Z^2) = 0.1165$ and $\alpha_s(m_Z^2) = 0.1195$, and that can be used for the computation of the combined PDF+α_s uncertainties, as explained in Sect. 6.2. Finally, for ease of usage, the combined sets for $\alpha_s(m_Z^2) = 0.118$ are also presented bundled with the α_s-varying sets in dedicated grid files. The specifications of each of the combined NNLO PDF4LHC15 sets that are available from LHAPDF6 are summarized in Table 5; note that the corresponding NLO sets are also available.

Usage of the PDF4LHC15 sets. As illustrated in Sect. 5, the three delivery options provide a reasonably accurate representation of the original prior combination. However, each of these methods has its own advantages and disadvantages, which make them more suited in different specific contexts. We now attempt to provide some general guidance about which of the three PDF4LHC15 combined sets should be used in specific phenomenological applications.

1. **Comparisons between data and theory for Standard Model measurements**

   Recommendations: Use *individual PDF sets*, and, in particular, as many of the modern PDF sets [5–11] as possible.

   Rationale: Measurements such as jet production, vector-boson single and pair production, or top-quark pair production, have the power to constrain PDFs, and this is best utilized and illustrated by comparing with many individual sets.

   As a rule of thumb, *any measurement that potentially can be included in PDF fits* falls in this category.

   The same recommendation applies to the *extraction of precision SM parameters*, such as the strong coupling $\alpha_s(m_Z^2)$ [75, 124], the W mass M_W [125], and the top quark mass m_t [126] which are directly correlated to the PDFs used in the extraction.

2. **Searches for Beyond the Standard Model phenomena**

   Recommendations: Use the PDF4LHC15_mc sets.

   Rationale: BSM searches, in particular for *new massive particles in the TeV scale*, often require the knowledge of PDFs in regions where available experimental constraints are limited, notably close to the hadronic threshold where $x \to 1$ [127]. In these extreme kinematical regions the PDF uncertainties are large, the *Monte Carlo combination of PDF sets is likely to be non-Gaussian. c.f.* Figs. 10 and 11.

47

The PDF4LHC document contains detailed guidelines to help decide which individual or combined PDFs to use depending on the circumstances

To assist in choosing the best PDF(s), demonstrative comparisons were generated of typical LHC cross sections for recent PDFs

1. **MC2H gallery of LHC cross sections:** ApplGrid, typical experimental cuts

www.hep.ucl.ac.uk/pdf4lhc/mc2h-gallery/

2. META gallery of LHC cross sections: ApplGrid or full calculations, minimal cuts

Metapdf.hepforge.org/2016_pdf4lhc/

Averaging of PDF ensembles

The 2012 recommendation estimated the combined uncertainty as an envelope of **cross sections** for 3 PDF sets; the envelope was overly sensitive to outliers

By 2015, several methods for combination (averaging) of **PDFs** (before computing cross sections) were developed. Criteria allowing the combination were outlined.

Combination workflow:

1. Generate 900 MC replicas from all input ensembles (currently CT14, MMHT14, NNPDF3.0) using Thorne-Watt procedure

   Other PDF sets can be added in the future if they satisfy the listed criteria

2. Reduce the number of final replicas from 900 to 100 or 30 by keeping most relevant PDF combinations

Reduced sets

- 900 error PDFs are too much for general use
- 3 reduction techniques have been developed
  - Compressed Monte Carlo PDFs (PDF4LHC15_nnlo(nlo)_mc)
    - 100 PDF error sets; preserve non-Gaussian errors
  - **META Hessian PDFs (PDF4LHC15_nnlo(nlo)_30**
    - 30 PDF error sets using METAPDF technique; Gaussian (symmetric) errors
  - MCH Hessian PDFs (PDF4lhc15_nnlo(nlo)_100
    - 100 PDF error sets using MCH technique; Gaussian (symmetric errors)
- The META technique is able to more efficiently reproduce the uncertainties when using a limited number (30) of error PDFs
- The MCH technique best reproduces the uncertainties of the 900 MC set prior

Comparisons of ensembles with 900, 100, 30 replicas

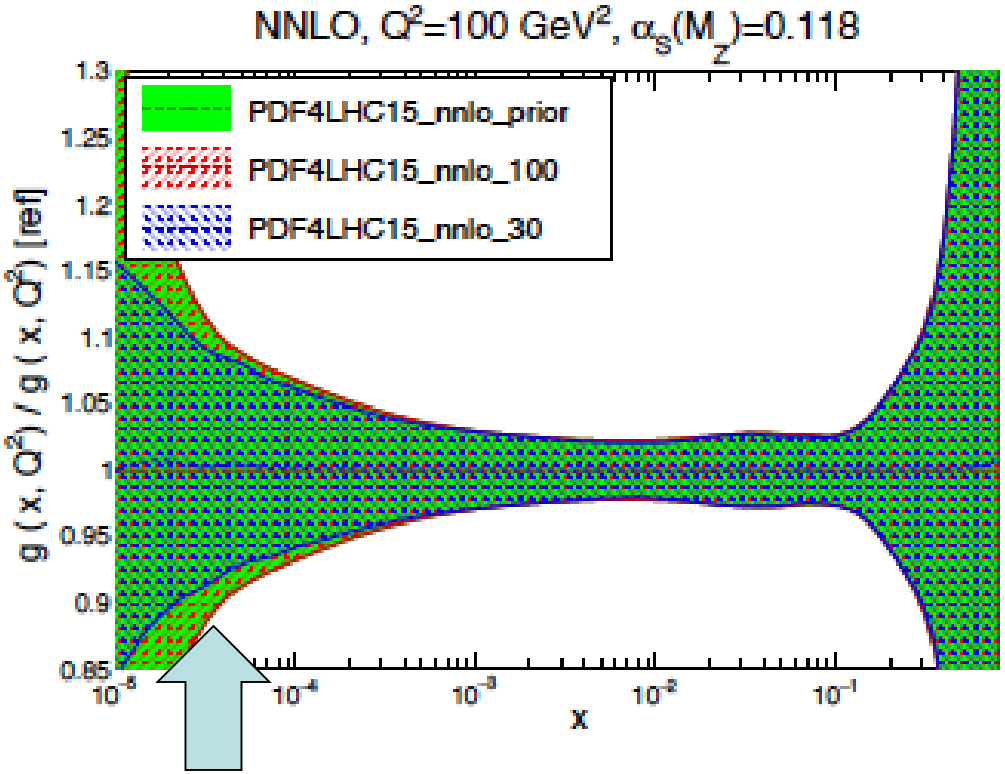

Three reduced PDF4LHC sets (100, MC, 30) reproduce well the 900-replica prior. Keep in mind that the uncertainty of the prior has an uncertainty of its own. By their construction, the lowest Hessian eigenvector sets are known the best, the highest sets are known with less confidence.

The 30-member ensemble keeps the lowest, best known sets and thus provides a lower estimate for the _900 prior uncertainty, known with higher confidence. When this estimate is not sufficient, or non-Gaussianities are important, use the 100 and MC sets

Ranges with differences between input PDFs, prior, and reduced sets

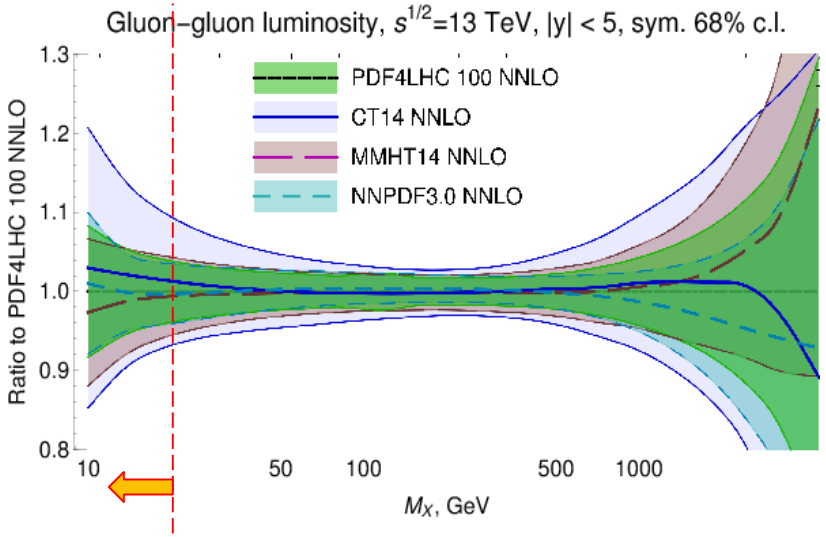

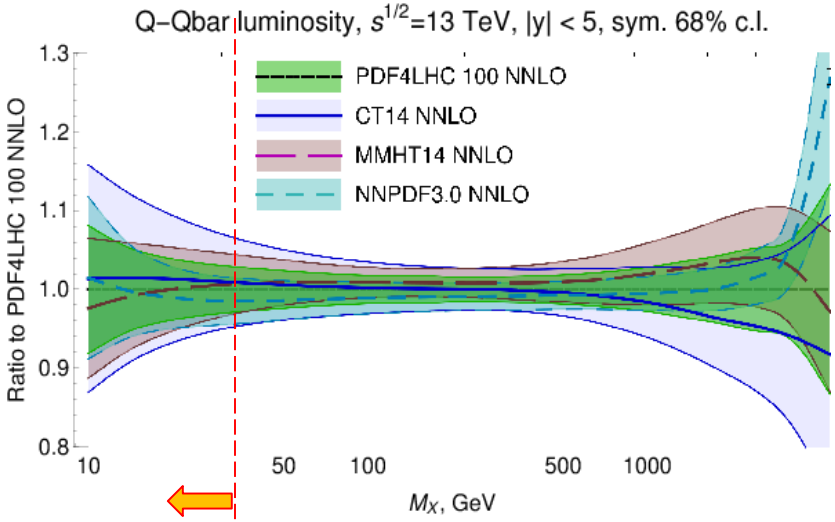

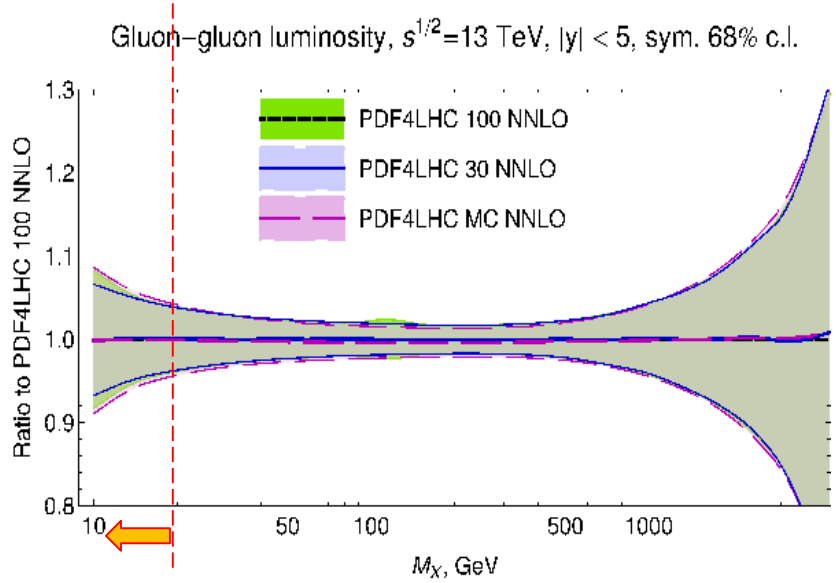

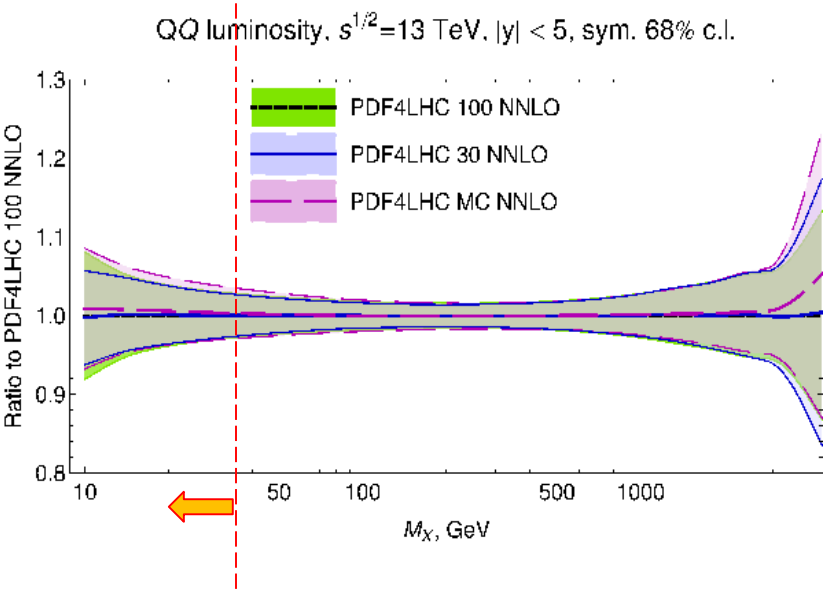

Note the $|y| < 5$ cut to constrain comparisons to the experimentally accessible region

Dependence of LHC observab...

metapdf.hepforge.org/2016_pdf4lhc/

Search

METAPDF is hosted by Hepforge, IPPP Durham

Dependence of LHC observables on parton distribution functions

CONTENTS

1. $p + p \to Z + X$

   [settings of the calculation] [Applgrid files]
   - PDF4LHC15 PDFs (NLO)
   - PDF4LHC15 PDFs (NNLO)
   - PDF4LHC15_100, HERA, ABM PDFs (NNLO)
   - PDF4LHC15_100, CT14, MMTH14, NNPDF3.0 PDFs (NNLO)

2. $p + p \to W^+ + X$

   [settings of the calculation] [Applgrid files]
   - PDF4LHC15 PDFs (NLO)
   - PDF4LHC15 PDFs (NNLO)

META gallery for basic processes at 7, 8, 13 TeV

Developed by Bo Ting Wang and Keping Xie

$p + p \to W^+ + X$

[settings of the calculation] [Applgrid files]

PDF4LHC15 PDFs (NLO)

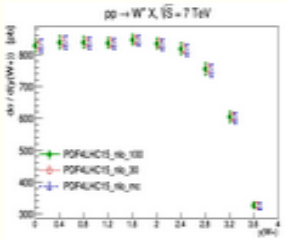
[pdf] [eps]

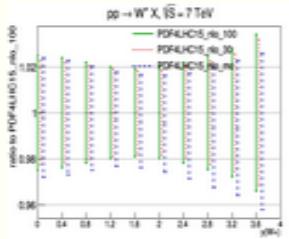
[pdf] [eps]

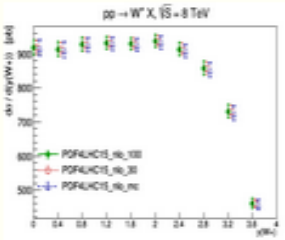
[pdf] [eps]

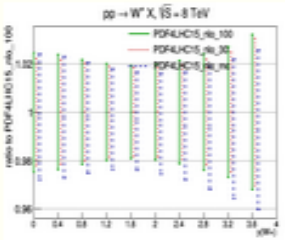
[pdf] [eps]

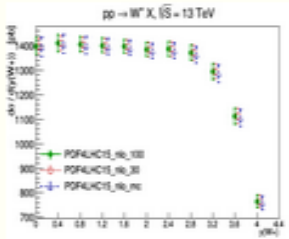
[pdf] [eps]

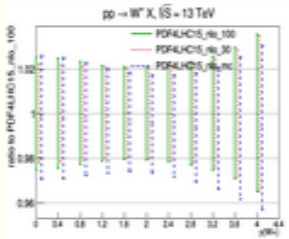
[pdf] [eps]

Gallery of phenomenological comparisons for LHC

Process	Order	Type of calculation
•p + p → Z + X	NLO	aMCFast/APPLgrid
•p + p → W^+ + X	NLO	aMCFast/APPLgrid
•p + p → W^- + X	NLO	aMCFast/APPLgrid
•p + p → $t\bar{t}$ + X	NLO	aMCFast/APPLgrid
•p + p → $t\bar{t}$ + X	NLO	aMCFast/APPLgrid
•p + p →$t\bar{t}\gamma\gamma$+X	NLO	aMCFast/APPLgrid
•ATLAS inclusive jets	NLO	NLOJET++/APPLgrid
•ATLAS inclusive dijets	NLO	NLOJET++/APPLgrid
•P + p → W^+ c + X	NLO	aMCFast/APPLgrid
•P + p → W^- c + X	NLO	aMCFast/APPLgrid
•P + p → H + X	LO,NLO	MCFM
•P + p → H+ jet + X	LO, NLO	MCFM

Compared PDFs: PDF4LHC15_100, _30, _MC, ABM'12, CT14, HERA2.0, MMHT14, NN3.0

Both full (MCFM) and fast (ApplGrid) calculations. AppGrlids are generated with minimal cuts and can be downloaded.

Cross sections and their relative differences due to PDFs are shown for most processes.

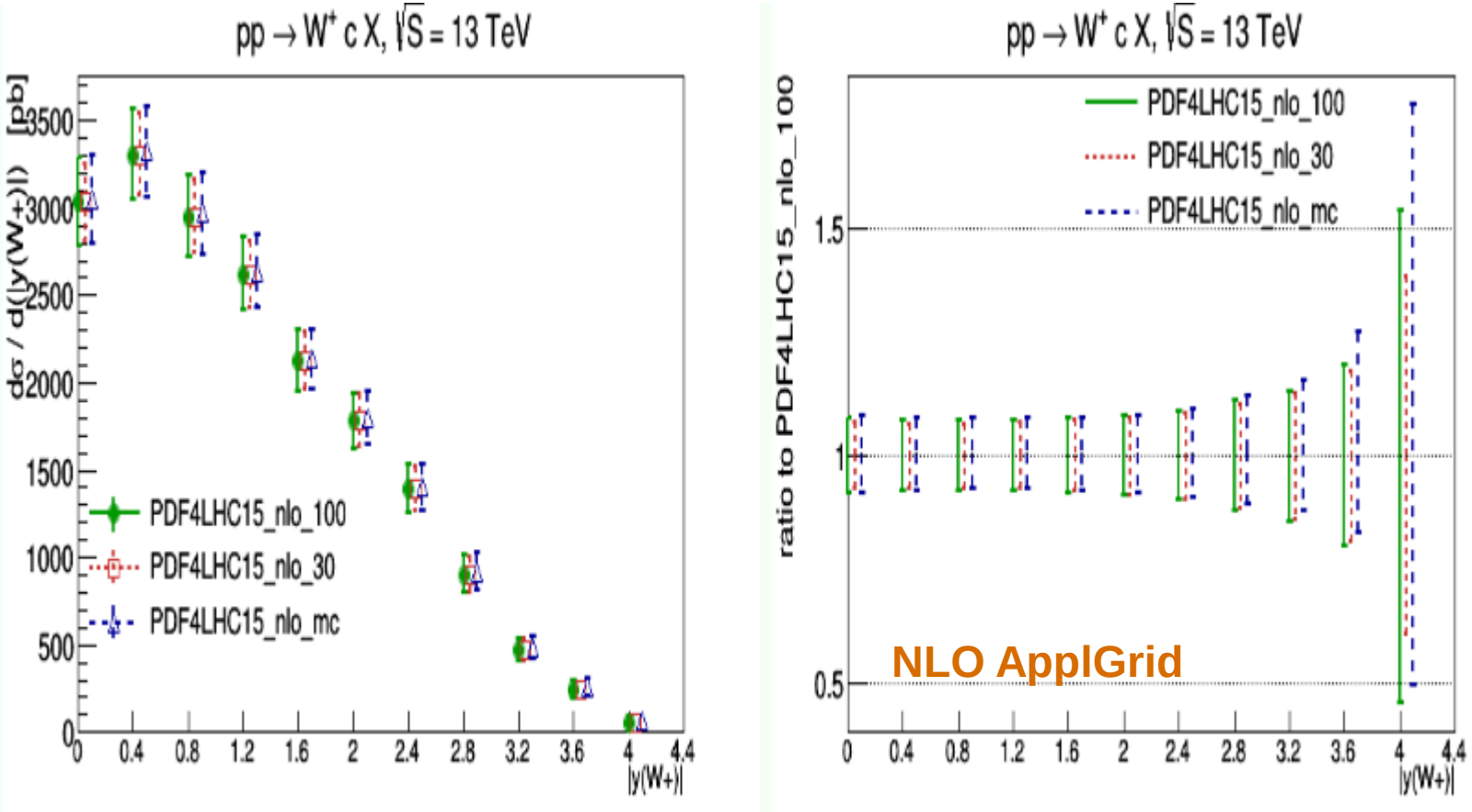

Relative differences tend to be larger when cross sections are small. Often they vary little across much of the range, can be eliminated by applying a constant rescaling factor (e.g., 1.05) to the PDF error.

MCFM: compare PDF and Monte-Carlo integration errors

Differences of PDF4LHC PDFs matter only when MC errors are negligible

PRELIMINARY

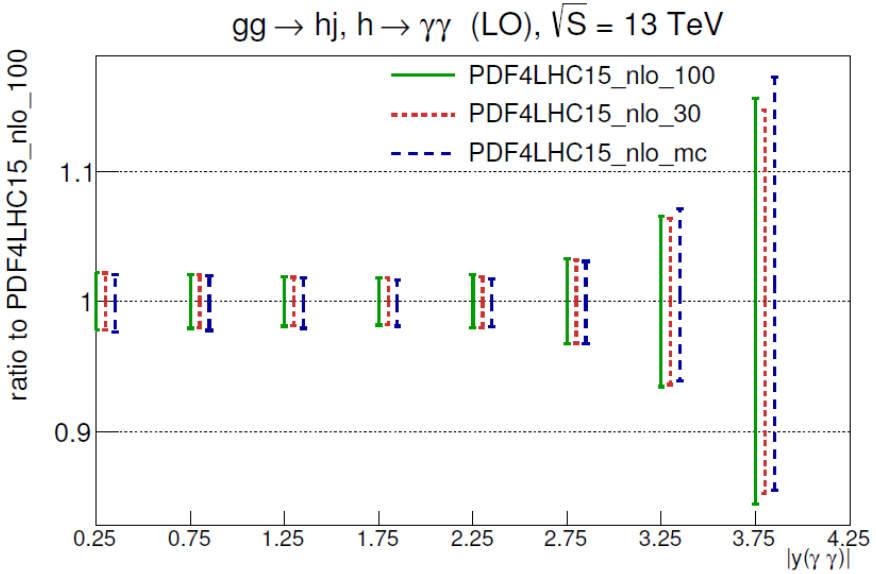

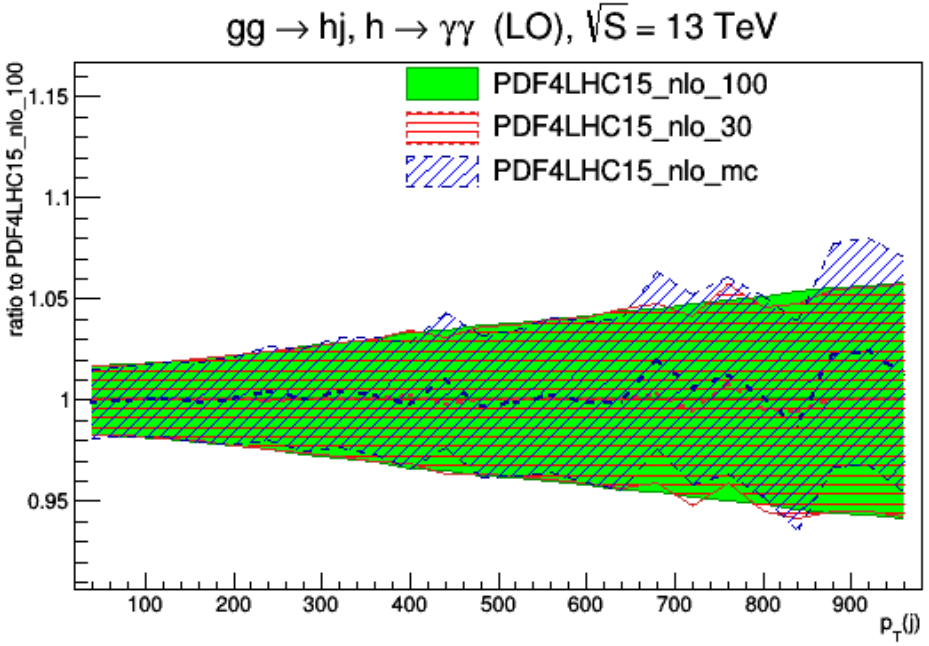

$gg \to H+j$ at LO.
10^6 events, ~1 hour per each PDF family

MC fluctuations in **central values** and PDF errors are often of the same order as the primordial differences

MC fluctuations can be suppressed by increasing the number of events or enlarging bin sizes. This example also touches on broader questions.

1. There are several ways for “averaging” the input PDF sets, e.g., because they use different evolution codes or round-offs

2. Without PDF reweighting, MC fluctuations are sensitive independently to every replica. They vary by the process, order of the calculation, etc.

3. Procedural adjustments made to reduce MC errors tend to wash out disparities due to PDF reduction methods

Looking into the future

High-luminosity LHC

- New (N)NNLO calculations likely to be completed
- Measurements of Higgs cross sections/couplings become limited by PDFs in the HL-LHC era
- Searches for non-resonant production in TeV mass range will demand accurate predictions for **sea** PDFs at $x > 0.1$

Projected Experimental Uncertainties

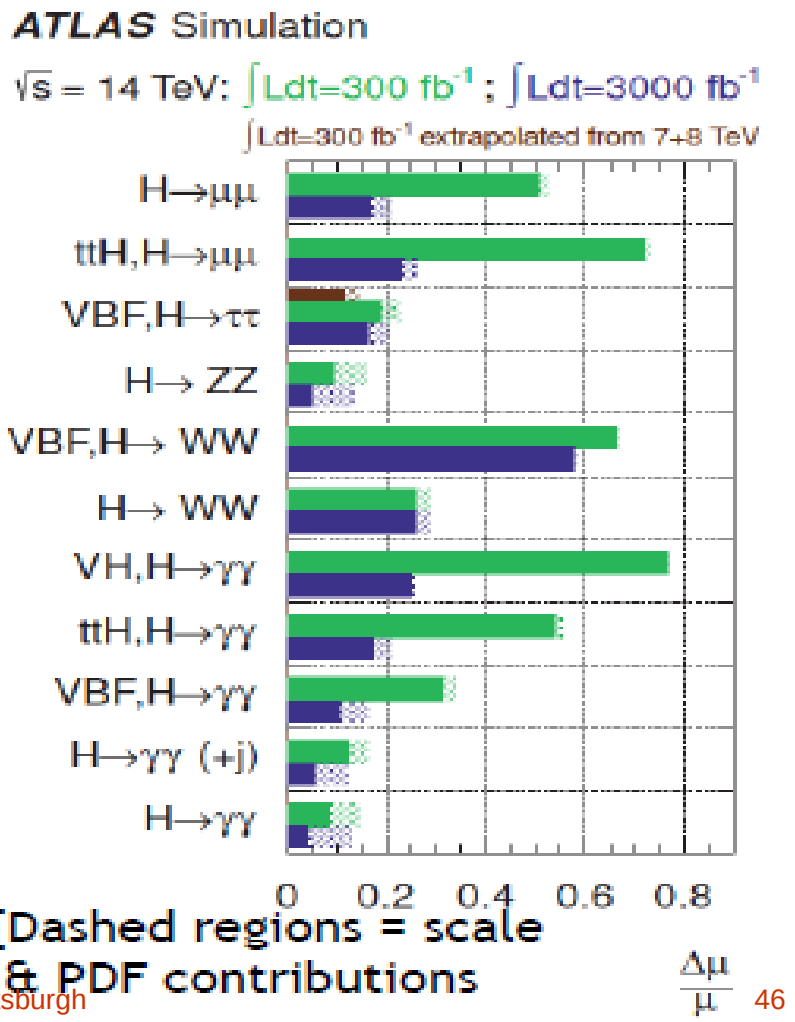

P. Newman, DIS'2016

Toward proton PDFs at 1% accuracy

Theory:

1. Development of efficient techniques to estimate PDF dependence at (N)NNLO
    a) Interfaces for fast (N)NLO computations *(Applgrid, FastNLO, aMCFast)*
    b) Combination at the PDF level *(META, CMC), reduced PDFs for classes of processes*
2. Inclusion of subleading effects (NLO EM corrections, photon PDFs, off-shell resonant production…) and theoretical uncertainties (scale dependence, heavy-quark schemes, …)
3. Advanced statistical methods (MC, reweighting…)
4. Special-purpose PDFs: for parton showering programs, with intrinsic charm, for resummations, …

Toward proton PDFs at 1% accuracy

Experiment:

1. Finding new, highly sensitive measurements for constraining PDFs
   a) Less inclusive, yet clean, processes *(e.g. Z p_T at NNLO…)*
   b) Better constraints at x>0.3
   c) Reliable flavor separation
2. Cross calibration of systematic uncertainties between the measurements
3. Smaller bin sizes, with some loss in statistics ⇒ better resolution on PDF x dependence

Thank you for your attention!

Backup slides

MMHT refit including combined HERA I+II data. Under refitting in global fit NLO – $\chi^2 = 1533/1185 = 1.29$ per point. NNLO – $\chi^2 = 1457/1185 = 1.23$ per point.

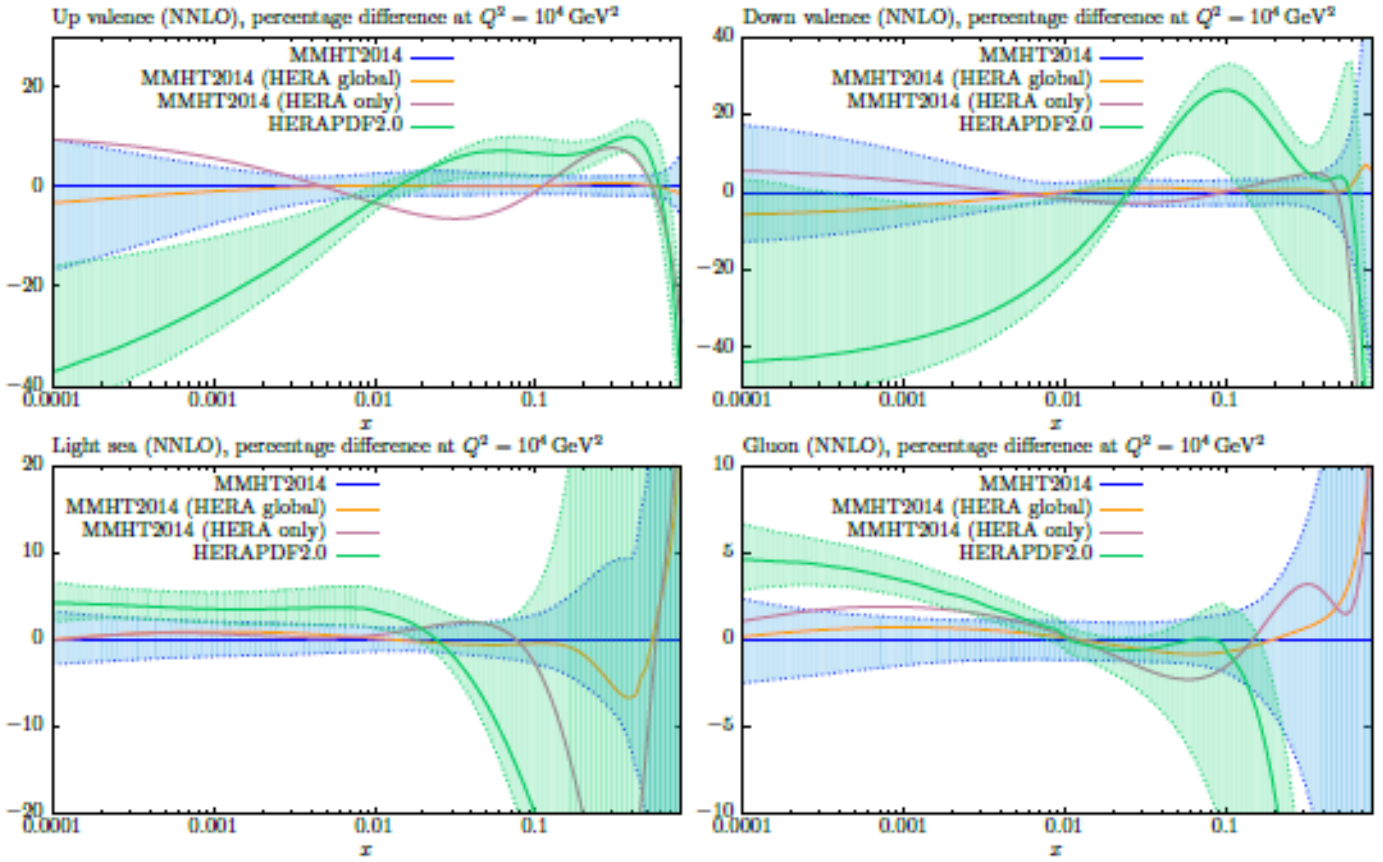

HERA II modified PDFs very well within MMHT2014 uncertainties. PDFs from HERA II data only fit in some ways similar to HERAPDF2.0.

R. Thorne

Modifications to the HERAPDF2.0 fit called HHT

By I.Abt, **A.M.Cooper-Sarkar**, B.Foster, V.Myronenko, K.Wichmann, M.Wing

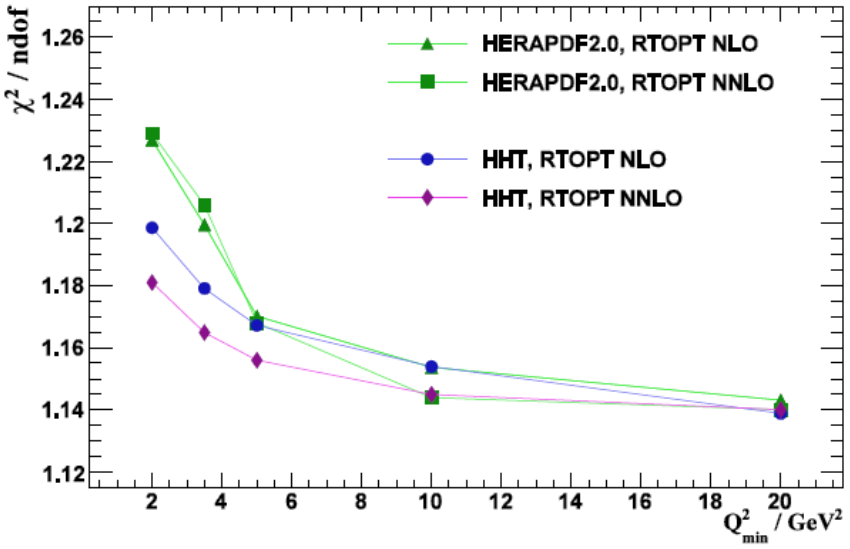

$$F_{2,L} = F_{2,L}\,(1 + A_{2,L}{}^{HT}/Q^2)$$

Addition of Higher Twist terms

- requires only modification of F_L
- and is only important for low-x

Greatly improves the description of low-Q^2, low-x and high-y data particularly at NNLO

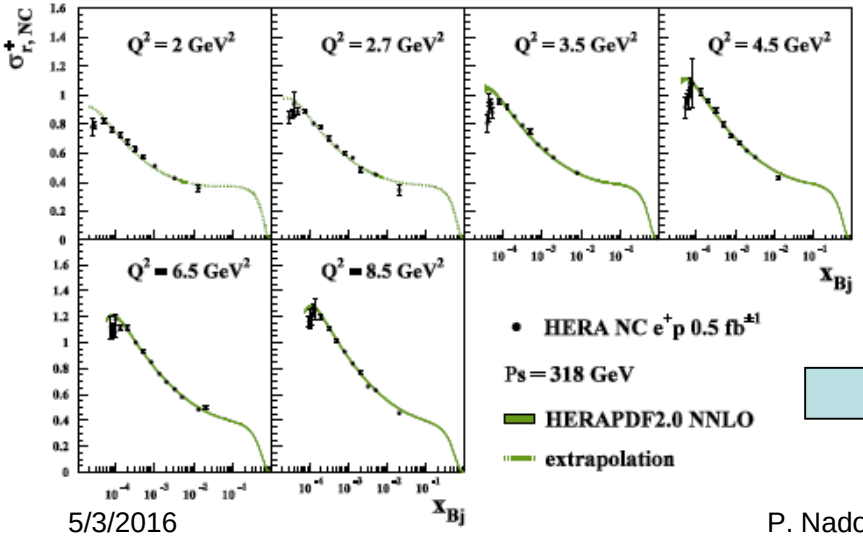

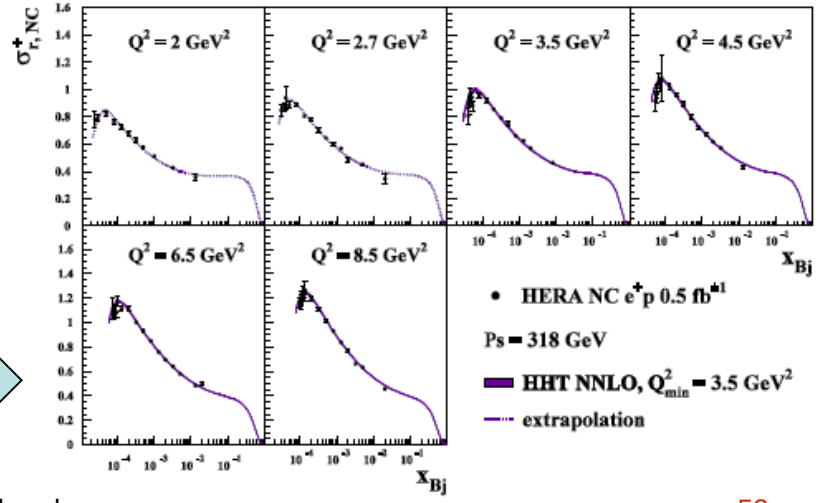

PDFs – and hence high Q^2 physics - not changed

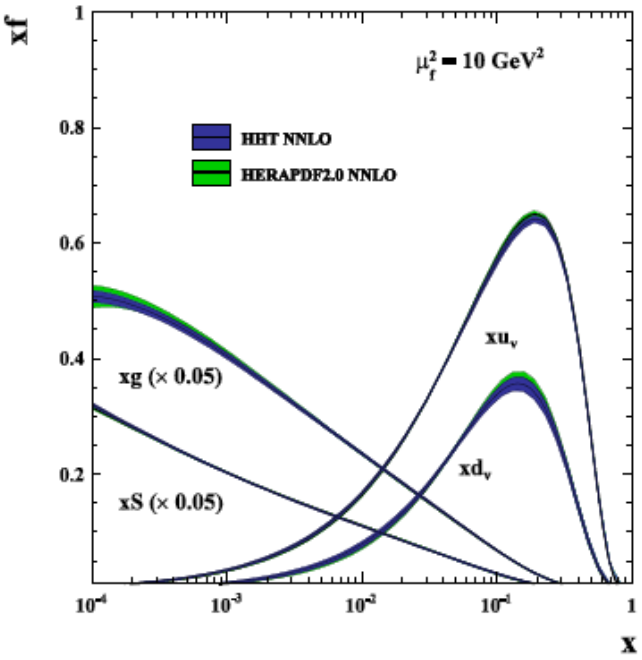

Predicted FL - compared to the measured FL from H1 and ZEUS – is enhanced for $Q^2 < 50\ \mathrm{GeV}^2$.

However it is clear that this approach cannot be pushed to very low $Q^2 < \sim 2\ \mathrm{GeV}^2$

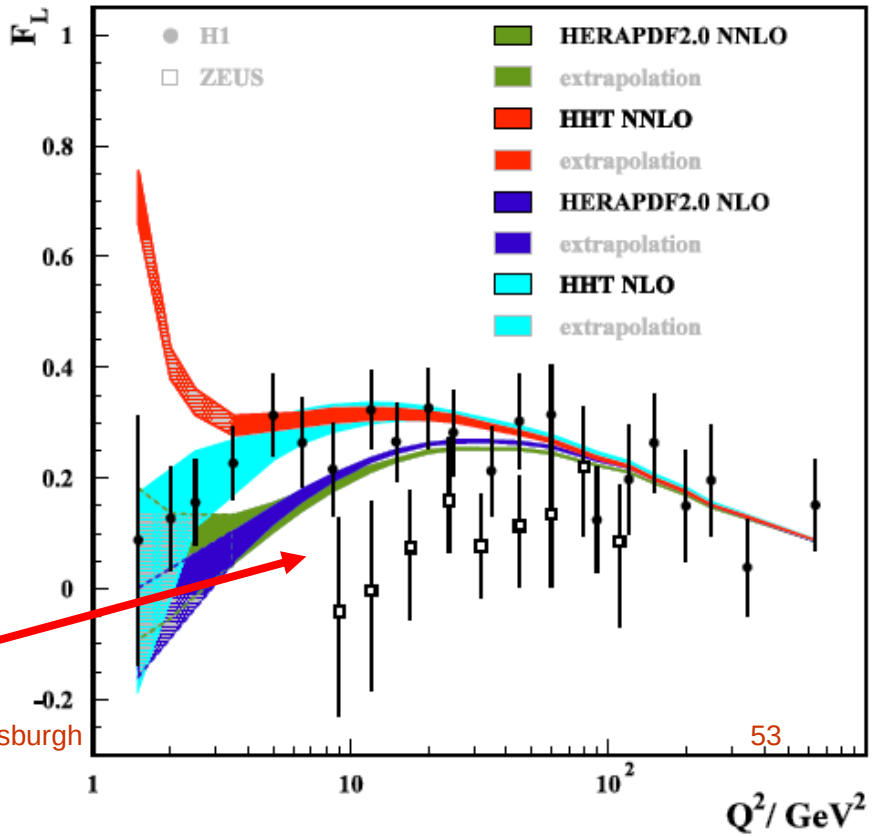

P.N.: Notice differences between H1 and ZEUS

Specialized PDF sets

CJ15: DIS data for $Q^2 > 1.3\ GeV^2$, $W^2 > 3\ GeV^2$

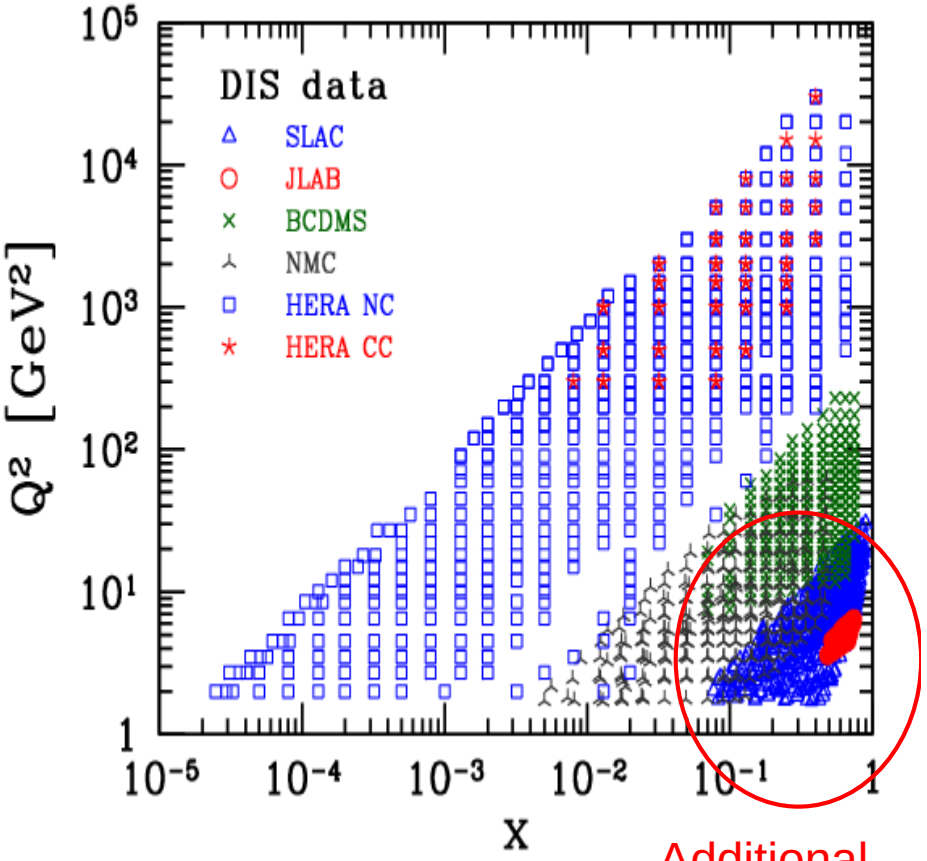

Additional constraints on d/u

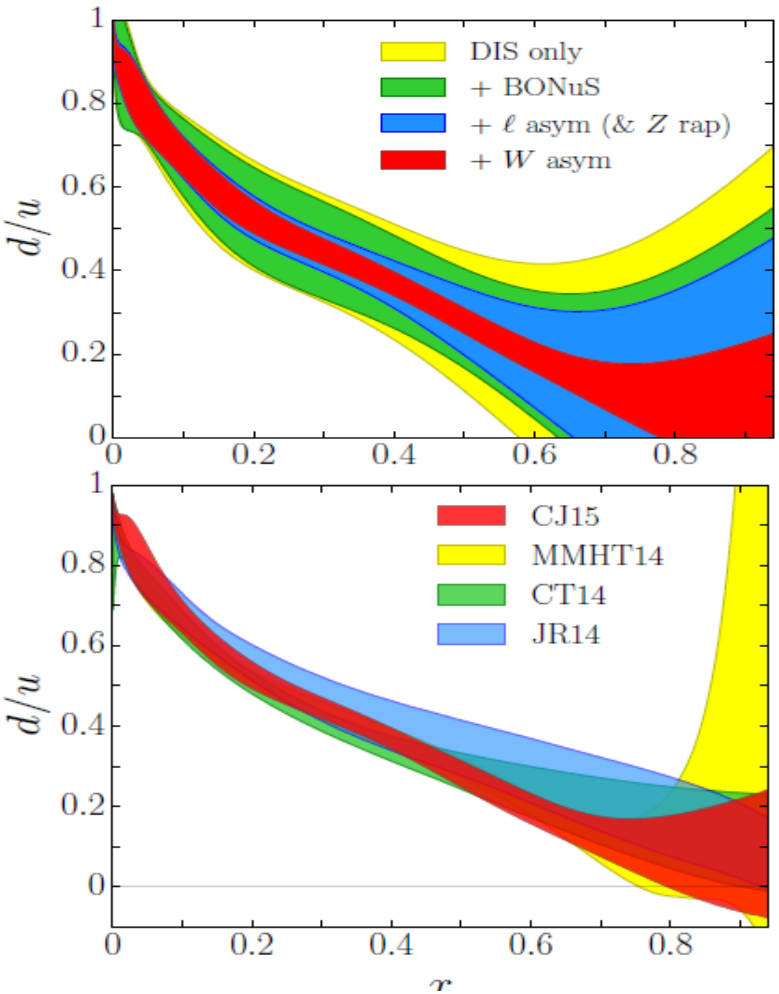

FIG. 16: Comparison of the d/u ratio at $Q^2 = 10$ GeV^2 for different PDF parametrizations: CJ15 (red band), MMHT14 [6] (yellow band), CT14 [7] (green band), and JR14 [10] (blue band).

CJ15 vs. others

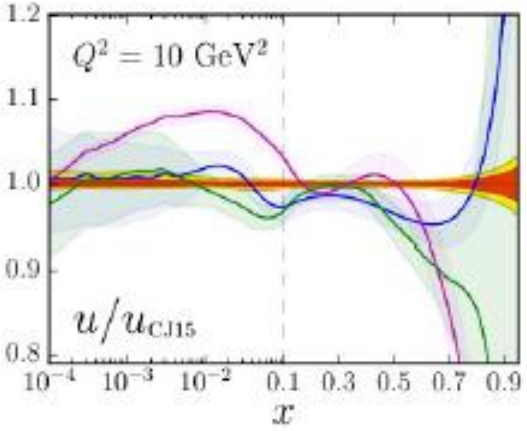

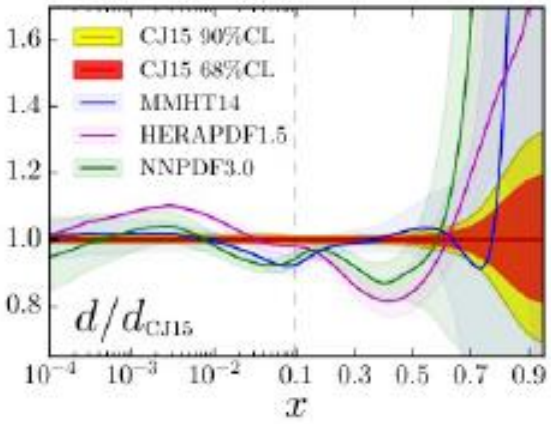

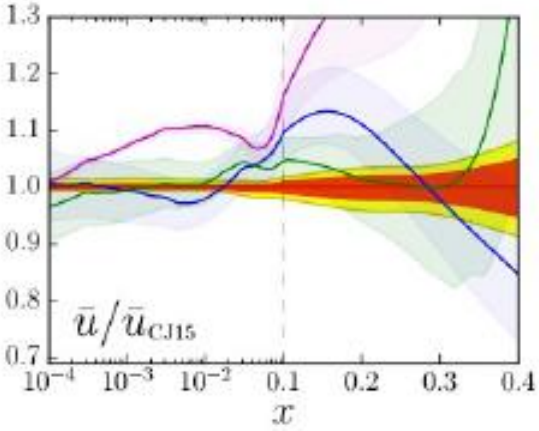

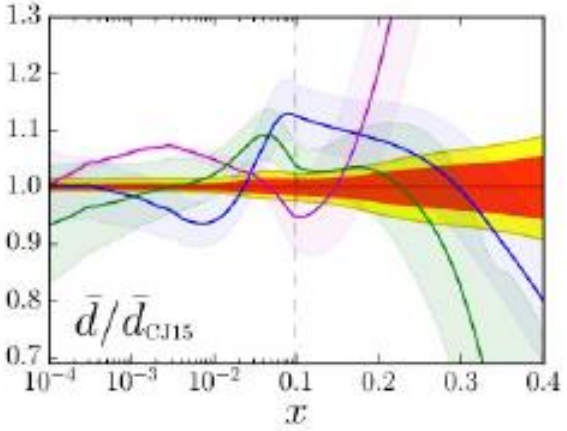

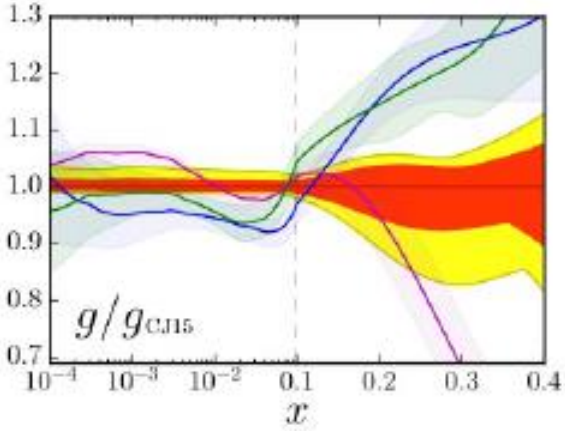

Various photon PDFs at Q=3.2 GeV

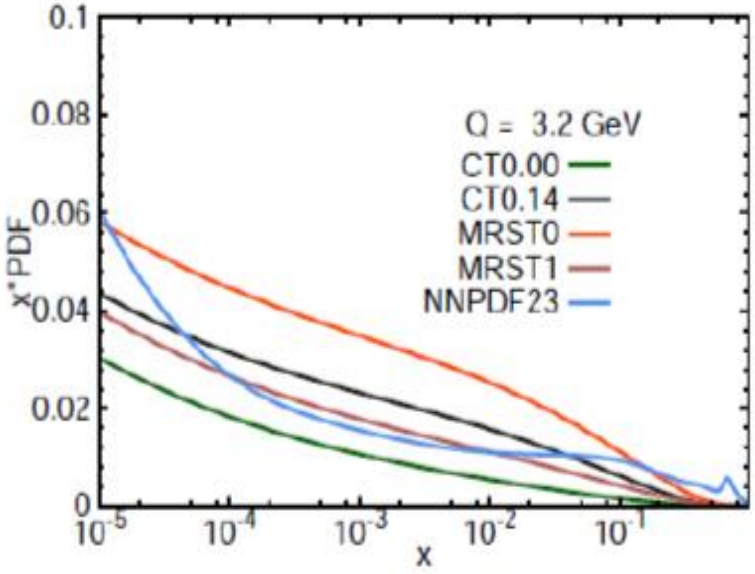

FIG. 10: Comparison of various NLO photon PDFs at the scale $Q = 3.2$ GeV: CT14QED with $p_0^\gamma = 0\%$ (green), CT14QED with $p_0^\gamma = 0.14\%$ (black), MRST2004QED0 using current quark masses (orange), MRST2004QED1 using constituent quark masses (brown), and NNPDF2.3QED with $\alpha_s = 0.118$ and average photon (blue).

Various photon PDFs at Q=85 GeV and 1 TeV

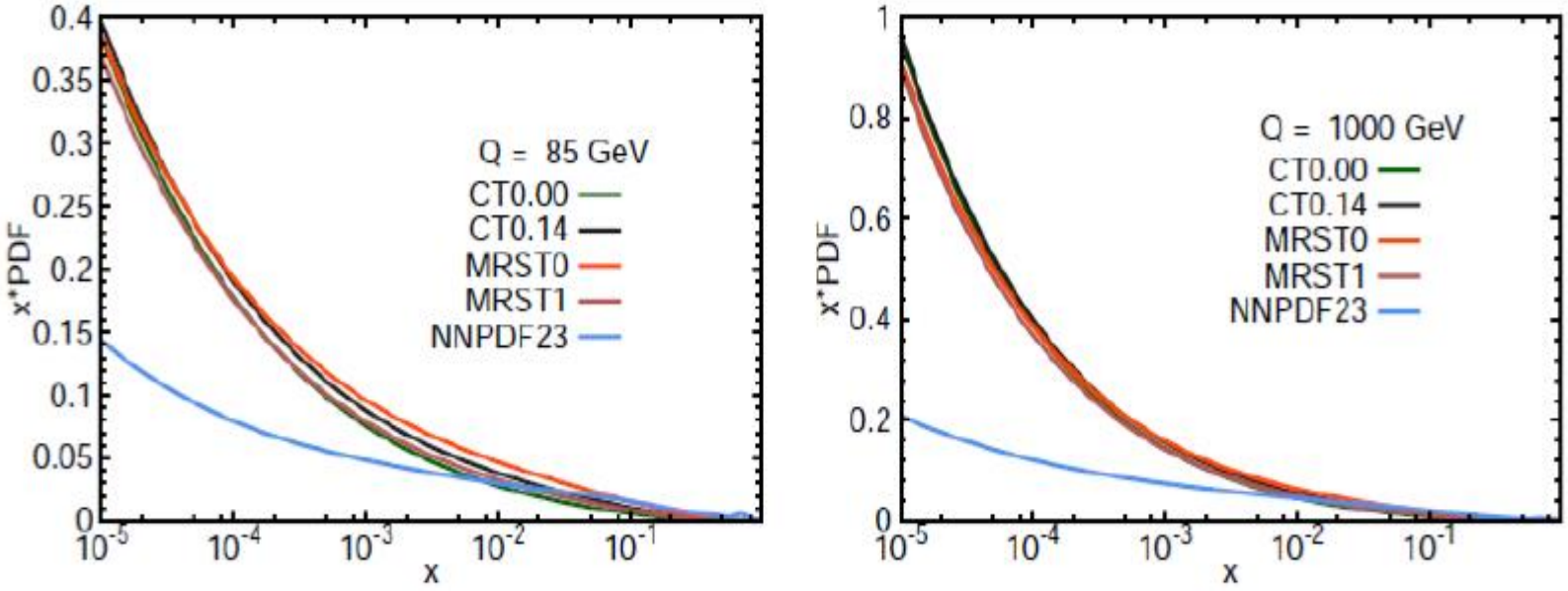

FIG. 11: Comparison of various NLO photon PDFs at the scales $Q = 85$ GeV (left) and $Q = 1$ TeV (right): CT14QED with $p_0^\gamma = 0\%$ (green), CT14QED with $p_0^\gamma = 0.14\%$ (black), MRST2004QED0 using current quark masses (orange), MRST2004QED1 using constituent quark masses (brown), and NNPDF2.3QED with $\alpha_s = 0.118$ and average photon (blue).

Photon-Photon Luminosity

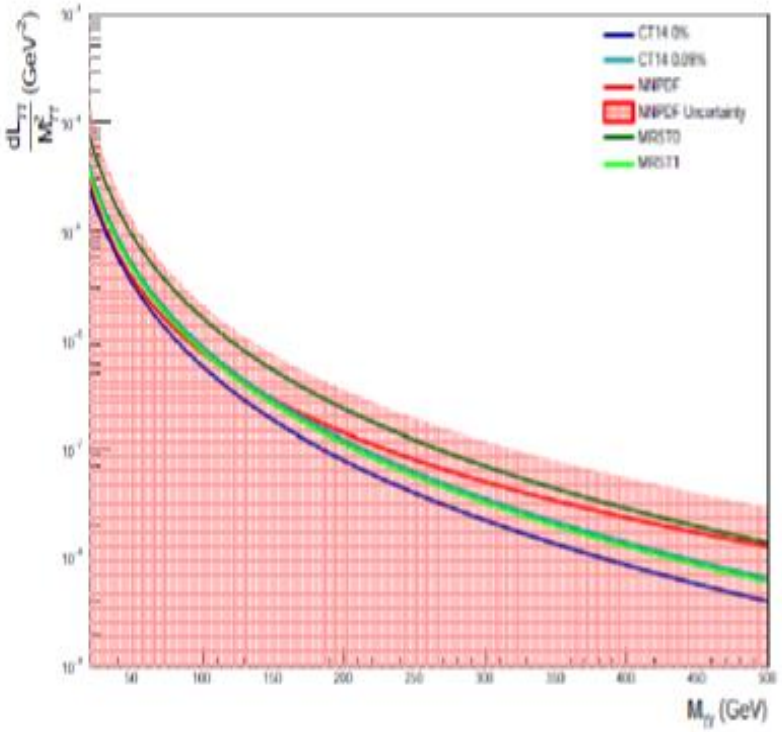

FIG. 4: Photon-photon luminosity for an invariant mass of 20 GeV to 500 GeV for 13 TeV collider energy

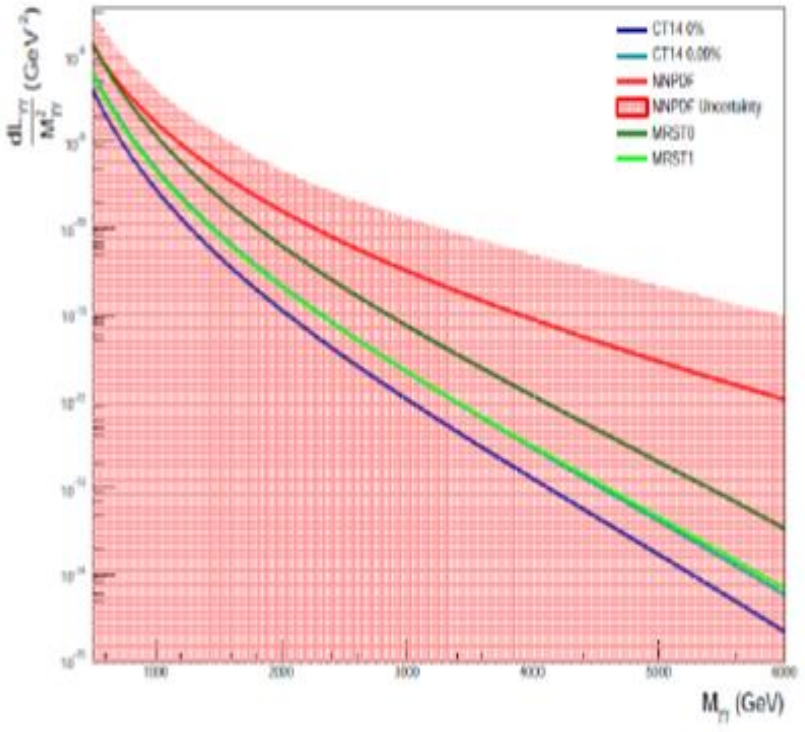

FIG. 5: Photon-photon luminosity for and invariant mass of 500 GeV to 6000 GeV for 13 TeV collider energy

High mass Drell-Yan: results and comparison to theory II/II

- The measured cross-sections are compared to theoretical predictions using a selection of recent PDFs.
- Theory uncertainties are larger than measurement uncertainties
  => potential for PDF constraints.
- Photon induced contribution reaches 15%.

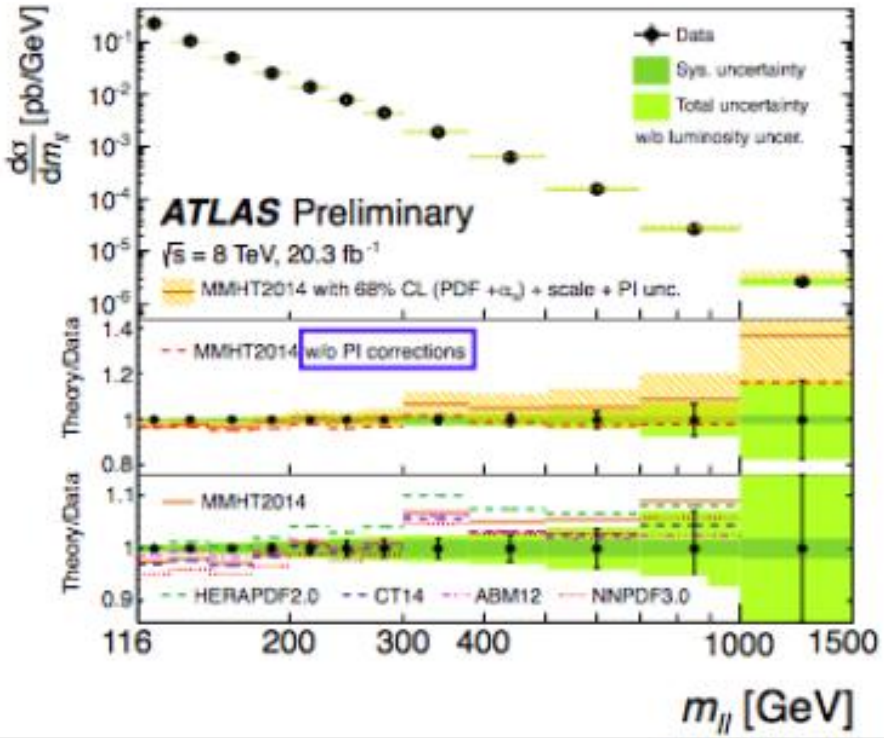

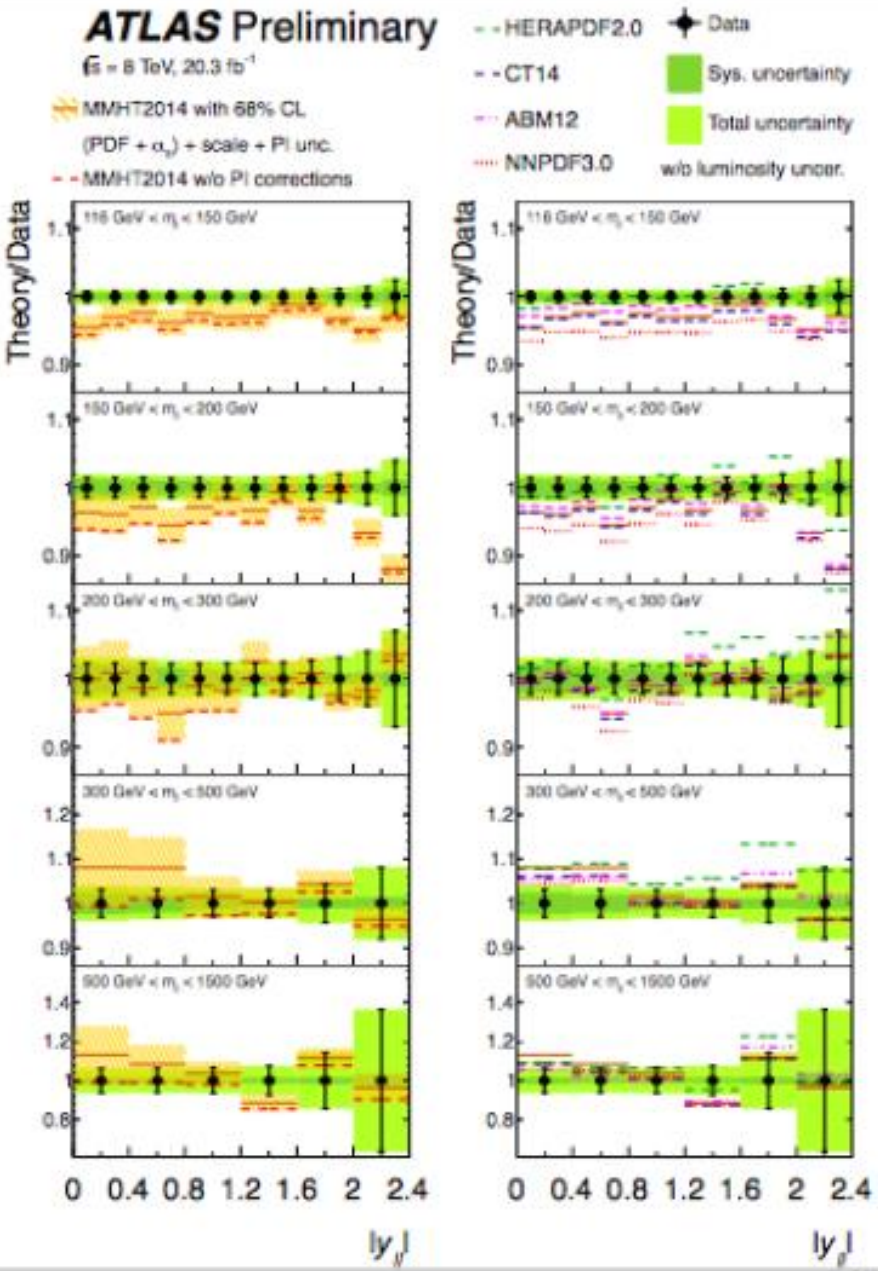

Compare CMS Data to various photon PDFs

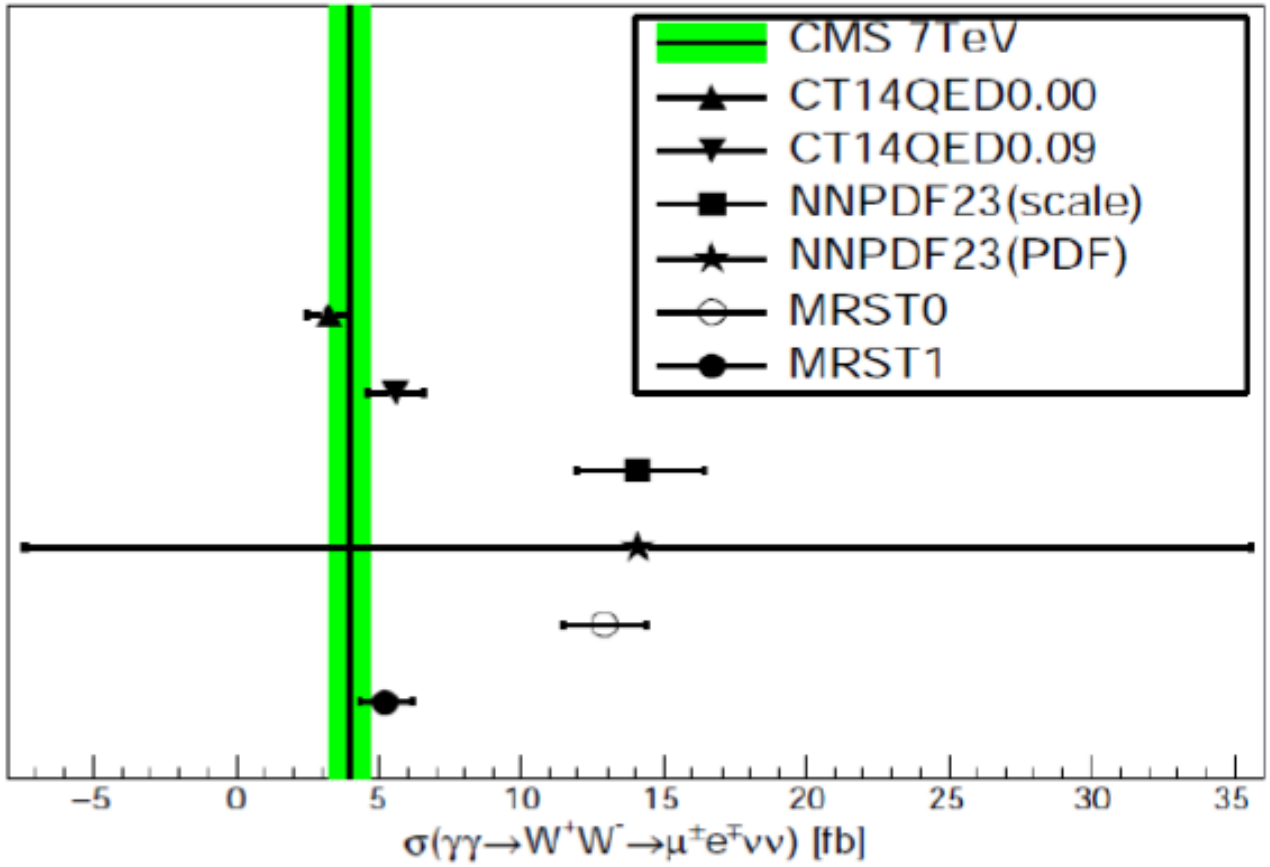

Intrinsic Charm PDFs from CTEQ-TEA Global Analysis

S. Dulat et al., 1309.0025; PoS DIS2015 (2015) 166

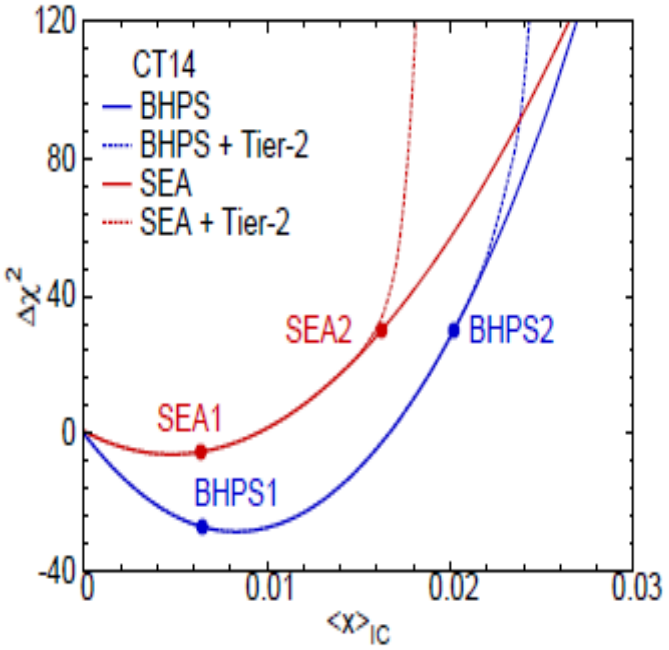

Figure 1: The $\Delta\chi^2$ versus the momentum fraction of charm $\langle x \rangle_{IC}$.

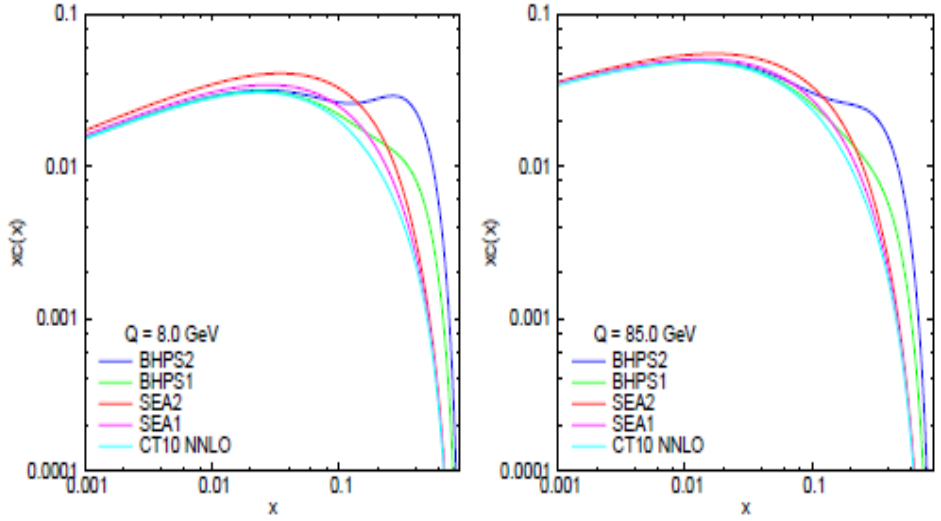

3. 3: Charm quark distribution $x\,c(x,Q)$ from the BHPS1 and BHPS2 PDFs (which have 0.57% and 2% $\langle x \rangle_{IC}$); from SEA1 and SEA2 PDFs (which have 0.57% and 1.5% $\langle x \rangle_{IC}$); and from CT10.

News from NNPDF (II)

- First determination of the **fitted charm PDF** in the NNPDF framework
- **Non-perturbative charm** can account for **up to 0.8% of the proton momentum** (68% CL)
- The **EMC charm structure function data** can be satisfactorily described
- Fitting the charm PDF stabilises the **m_c dependence of high-scale cross-sections**

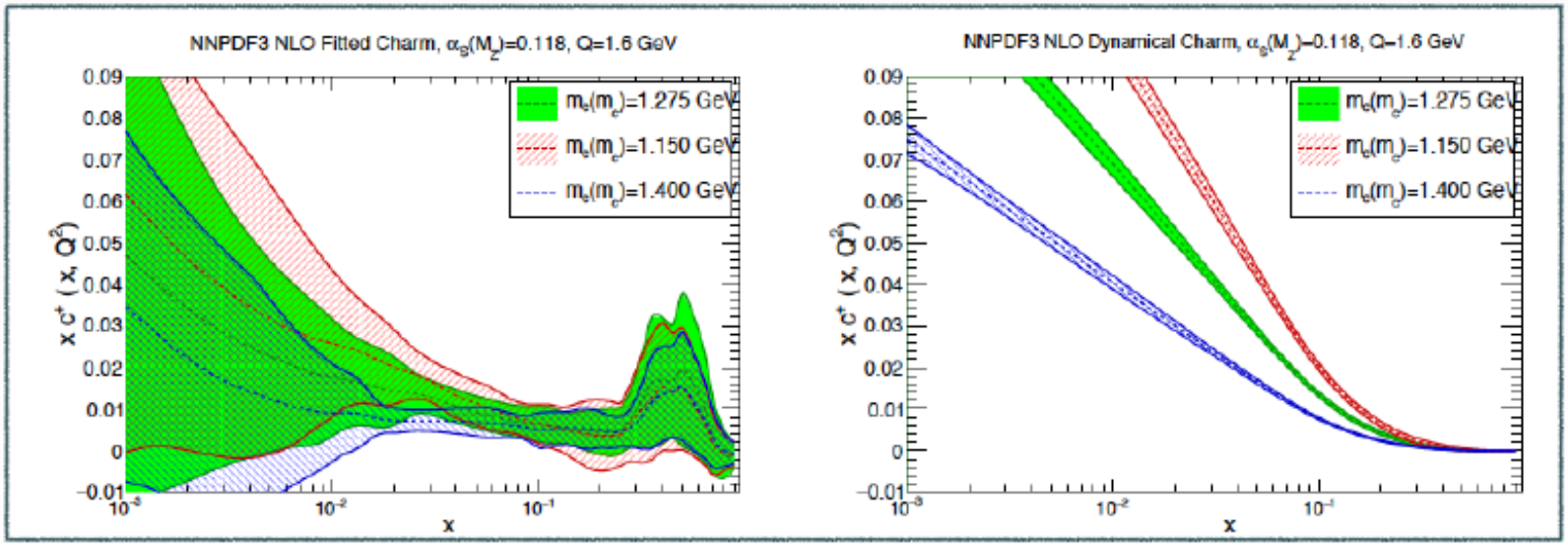

More in the talks from Juan Rojo (Tue) and Luca Rottoli (Wed)

Charm mass dependence of PDFs

NLO=$O(\alpha_s)$: GM-VFN predictions **for DIS** have large dependence on matching scales

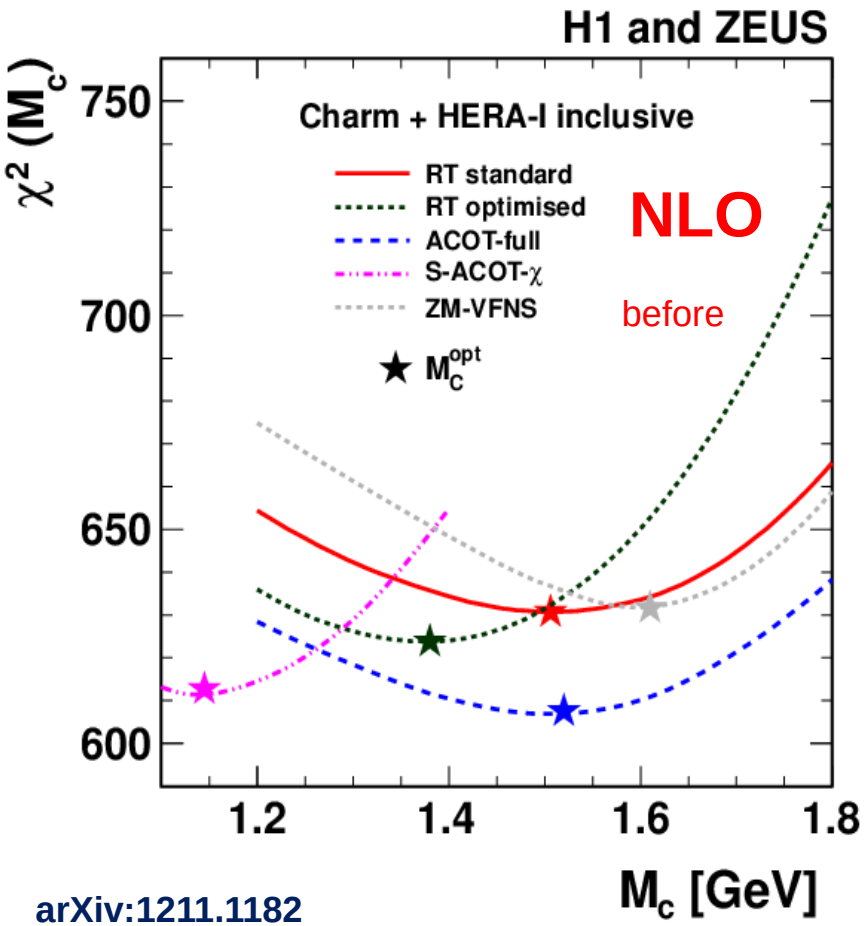

arXiv:1211.1182

The gluon PDF depends on the factorization scheme used to fit HERA DIS data

Besides the physical mass m_c, general-mass (GM-VFN) schemes used by global fits introduce matching energy scales of order m_c

At NLO, uncertainty due to matching parameters is large; each scheme prefers an "optimal" m_c that brings χ^2 to comparable levels (cf. the figure)

NNLO=$O(\alpha_s^2)$: dependence on matching parameters is suppressed, GM-VFN schemes are more similar

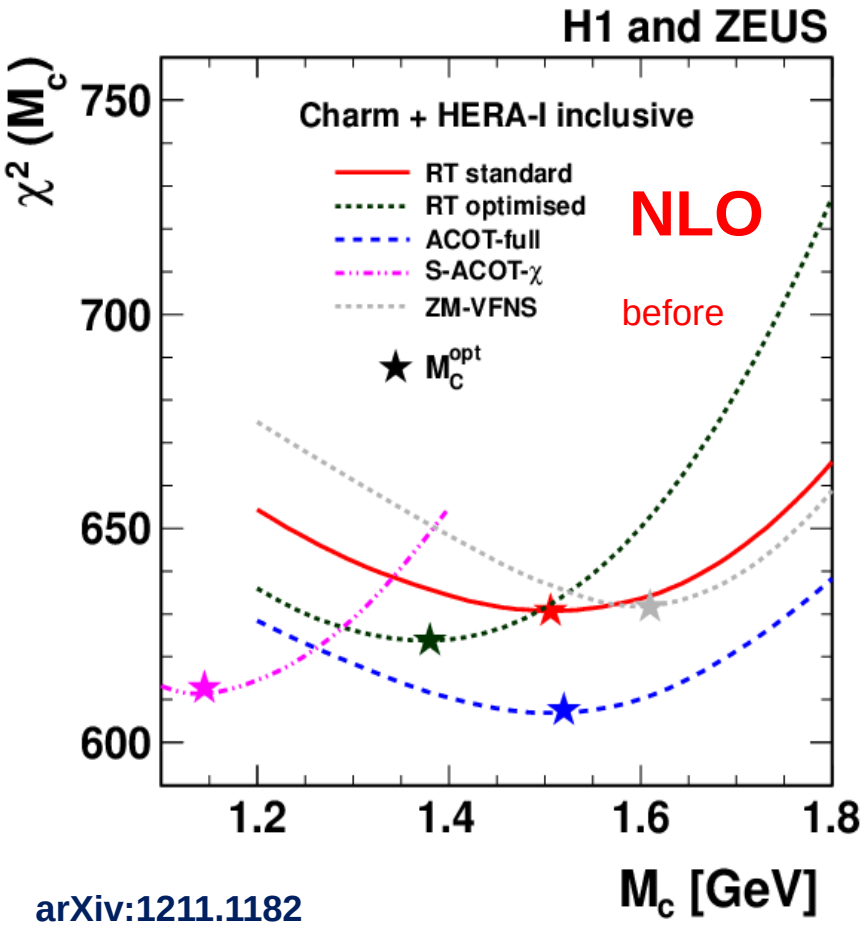

arXiv:1211.1182

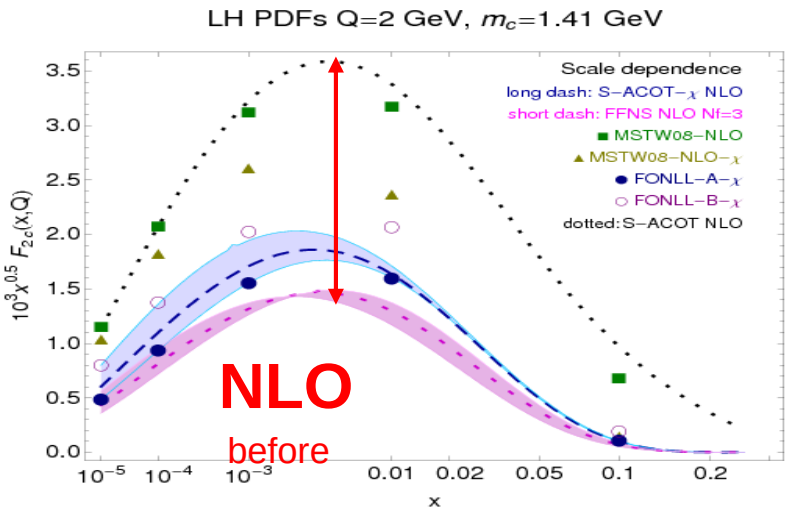

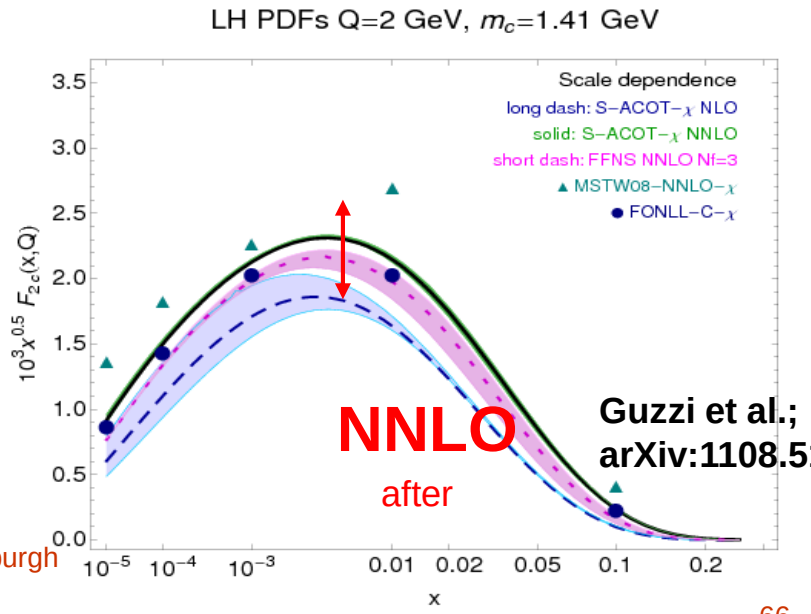

Guzzi et al.; arXiv:1108.5112

GM-VFN schemes are more predictive at NNLO

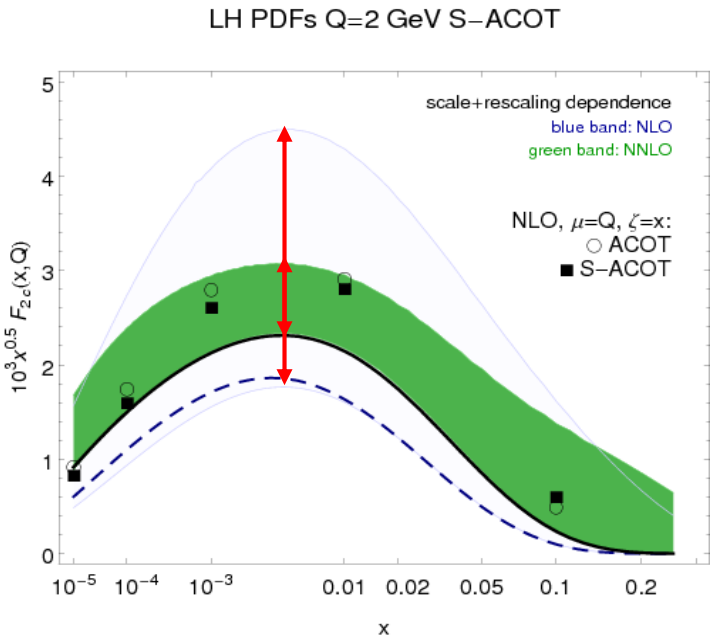

From Guzzi et al.; arXiv:1108.5112;
see also J. Rojo et al., 1003.1241, p. 110

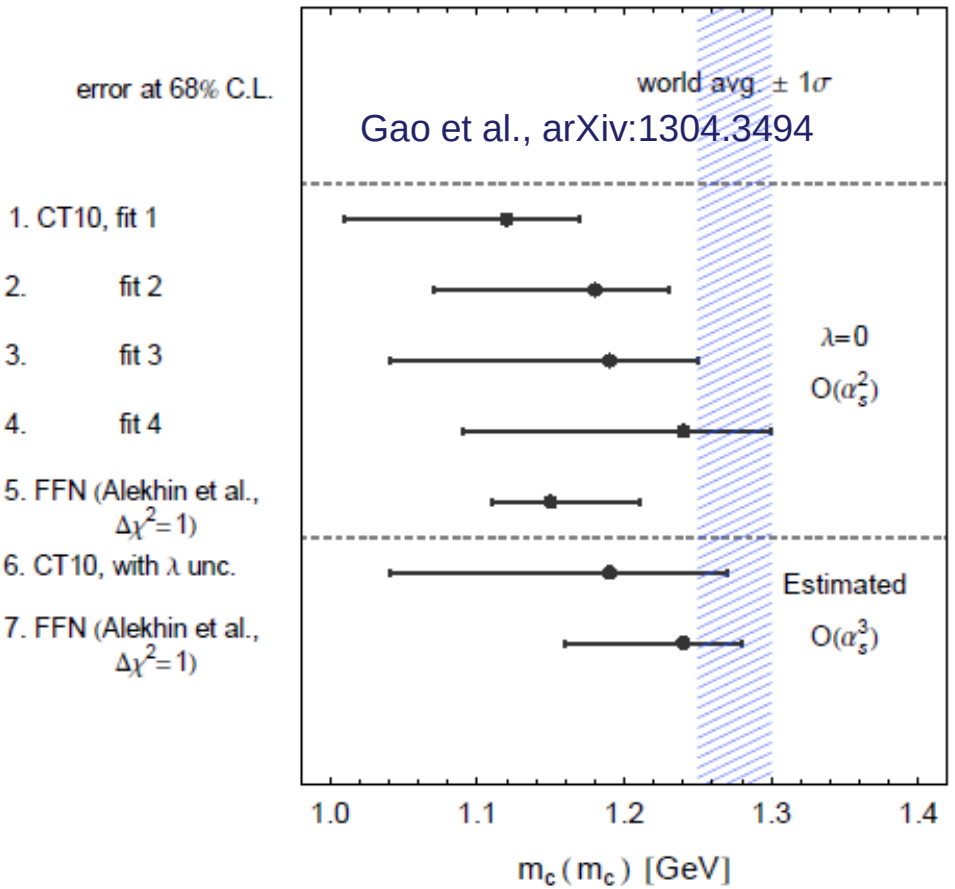

At $O(\alpha_s^2)$ and approximate $O(\alpha_s^3)$, constraints on $m_c(m_c)$ have been first obtained from combined HERA-I data in the FFN scheme (1212.2355) . Constraints on both m_c^{pole} or $m_c(m_c)$ in GM-VFNS have been also obtained by CT, MMHT, and NNPDF under varied assumptions. They are comparable with FFNS and the PDG value for $m_c(m_c)$.

Reduced META sets

Higgs eigenvector set

- For a given class of observables, the _30 set can be **diagonalized** to reproduce the bulk of the uncertainties and correlations with ~6 eigenvector sets

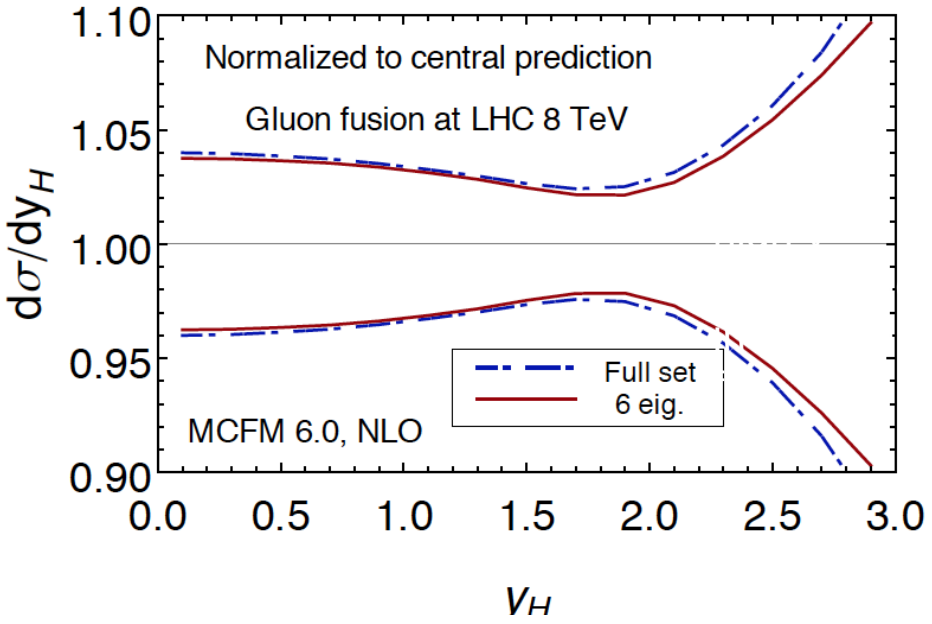

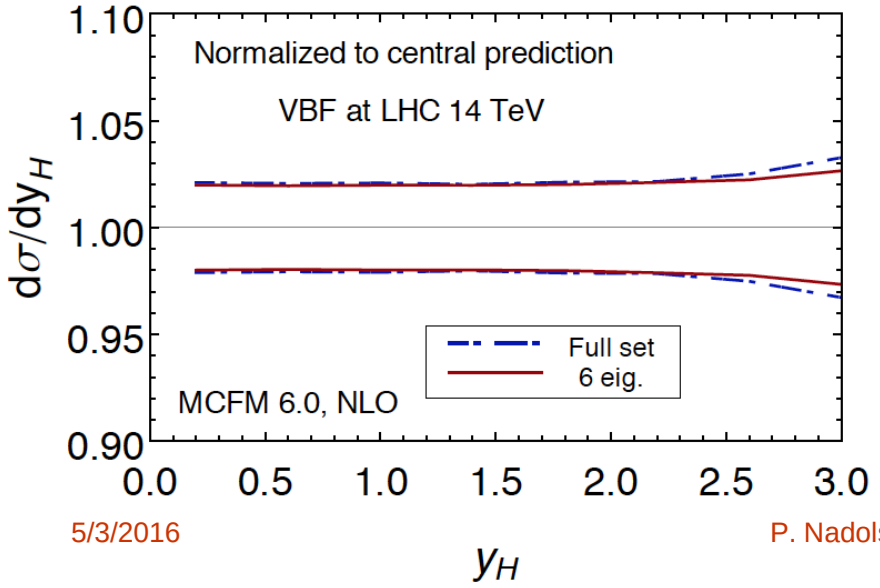

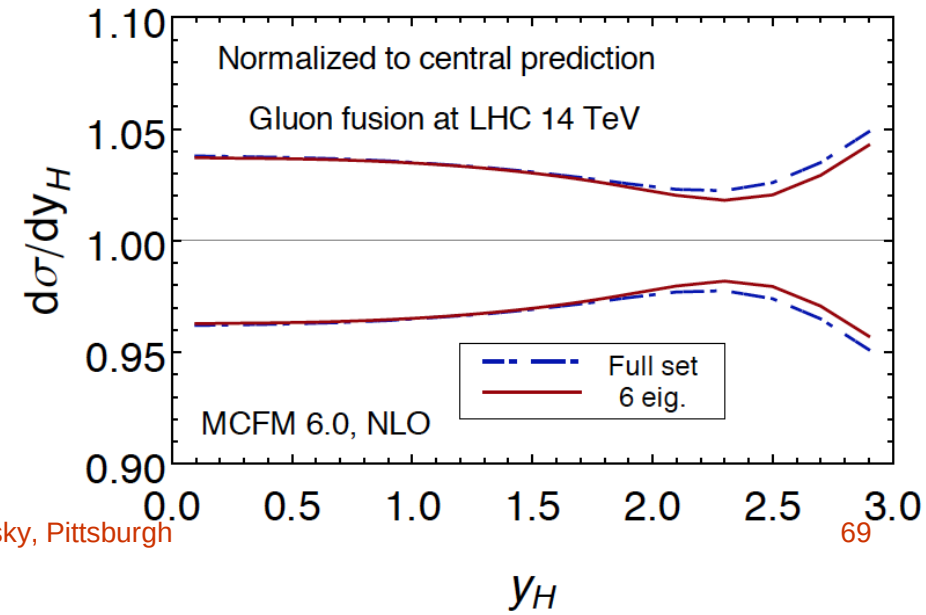

process	$\sigma_{cen.}$	δ_{Full}	$\delta_{Diag.}$	$\sigma^{\alpha_s}_{0.116}$	$\sigma^{\alpha_s}_{0.12}$
$gg \to H$ [pb]	18.77	$^{+0.48}_{-0.46}$	$^{+0.48}_{-0.44}$	18.11	19.4
	43.12	$^{+1.13}_{-1.07}$	$^{+1.13}_{-1.04}$	41.68	44.6
VBF [fb]	302.5	$^{+7.8}_{-6.7}$	$^{+7.6}_{-6.7}$	303.1	301.
	878.2	$^{+19.7}_{-17.9}$	$^{+19.2}_{-17.3}$	877.3	878.
HZ [fb]	396.3	$^{+8.4}_{-7.3}$	$^{+8.1}_{-7.4}$	393.0	399.
	814.3	$^{+14.8}_{-13.2}$	$^{+13.8}_{-13.0}$	806.5	823.
$HW^{\pm}$ [fb]	703.0	$^{+14.4}_{-14.4}$	$^{+14.3}_{-14.1}$	697.4	708.
	1381	$^{+28}_{-22}$	$^{+26}_{-22}$	1368	139
HH [fb]	7.81	$^{+0.33}_{-0.30}$	$^{+0.33}_{-0.30}$	7.50	8.1
	27.35	$^{+0.78}_{-0.72}$	$^{+0.78}_{-0.68}$	26.48	28.2
$t\bar{t}$ [pb]	248.4	$^{+9.1}_{-8.2}$	$^{+9.2}_{-8.1}$	237.1	259.
	816.9	$^{+21.4}_{-19.6}$	$^{+21.4}_{-18.4}$	785.5	848.
$Z/\gamma^*(l^+l^-)$ [nb]	1.129	$^{+0.025}_{-0.023}$	$^{+0.024}_{-0.023}$	1.113	1.14
	1.925	$^{+0.043}_{-0.041}$	$^{+0.040}_{-0.037}$	1.897	1.95
$W^+(l^+\nu)$ [nb]	7.13	$^{+0.14}_{-0.14}$	$^{+0.14}_{-0.13}$	7.03	7.25
	11.64	$^{+0.24}_{-0.23}$	$^{+0.22}_{-0.21}$	11.46	11.8
$W^-(l^-\bar{\nu})$ [nb]	4.99	$^{+0.12}_{-0.12}$	$^{+0.12}_{-0.11}$	4.92	5.08
	8.59	$^{+0.21}_{-0.20}$	$^{+0.19}_{-0.18}$	8.46	8.74
W^+W^- [pb]	4.14	$^{+0.08}_{-0.08}$	$^{+0.08}_{-0.07}$	4.04	4.20
	7.54	$^{+0.15}_{-0.14}$	$^{+0.14}_{-0.12}$	7.39	7.57
ZZ [pb]	0.703	$^{+0.016}_{-0.014}$	$^{+0.015}_{-0.014}$	0.695	0.71
	1.261	$^{+0.026}_{-0.024}$	$^{+0.024}_{-0.022}$	1.256	1.27
W^+Z [pb]	1.045	$^{+0.019}_{-0.018}$	$^{+0.019}_{-0.017}$	1.039	1.06
	1.871	$^{+0.033}_{-0.031}$	$^{+0.029}_{-0.027}$	1.850	1.89
W^-Z [pb]	0.788	$^{+0.020}_{-0.019}$	$^{+0.019}_{-0.018}$	0.780	0.79
	1.522	$^{+0.034}_{-0.032}$	$^{+0.033}_{-0.031}$	1.509	1.54

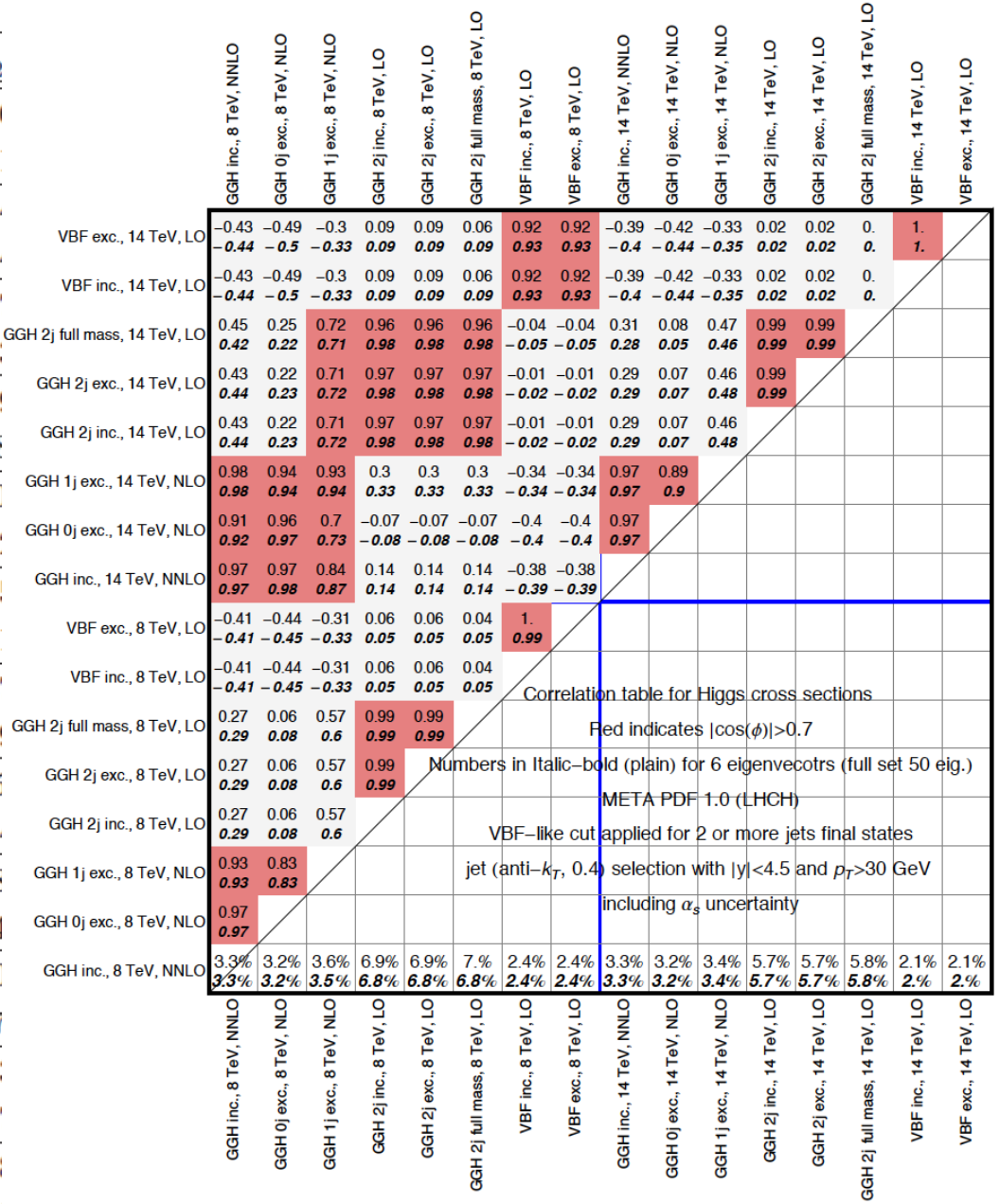

FIG. 7: Same as Fig. 5, with α_s uncertainties included by adding in quadrature.